STUDY OF MATHEMATICAL MODELS OF RADIOTHERAPY

Thesis
Submitted to the University of Calicut
for the award of Degree of
DOCTOR OF PHILOSOPHY IN PHYSICS

By

SANTHOSH V.S.

DEPARTMENT OF PHYSICS
UNIVERSITY OF CALICUT
KERALA, INDIA

MARCH 2008

CERTIFICATE

Certified that the thesis entitled "**STUDY OF MATHEMATICAL MODELS OF RADIOTHERAPY**" is a bonafide record of work done by **Mr. SANTHOSH V.S.** under my supervision in the Department of Physics, University of Calicut, and that no part of it has been included any were previously for the award of any degree.

Date:

Dr. B.R.S. BABU
Professor,
Department of Physics
University of Calicut

DECLARATION

I hereby declare that the thesis entitled "**STUDY OF MATHEMATICAL MODELS OF RADIOTHERAPY**" is an authentic record of the research work carried out by me under the supervision of **Dr. B.R.S. BABU**, Professor, Department of Physics, University of Calicut. No part of this thesis has formed the basis for the award of any other degree or diploma of any University or Institution.

Date: **SANTHOSH V.S.**

ACKNOWLEDGEMENTS

First and foremost, I would like to express my deepest gratitude to ***Dr. B.R.S. Babu****, Professor of Physics, University of Calicut, for his support and guidance as my Research Guide. Without his help, this work could not have been accomplished.*

I also would like to thank ***Dr.K.M. Varrior*** *Professor and Head, Department of Physics, University of Calicut for his support and providing facilities for conducting the research.*

I am forever indebted to ***Dr. K.V. Subbaiah****, Head, Safety Research Institute, IGCAR, Kalpakkam for his unconditional and selfless help.*

I would like to thank ***Dr. Suresh Babu****, Chief, Division of Radiation Physics, Department of Radiotherapy, Medical College, Trivandrum for his cooperation and moral support throughout the work.*

I also would like to thank ***Dr. R. Gireesan****, Head of Department of Radiotherapy, Medical College, Trivandrum for permitting me to do the research.*

I also thankful to ***Mr Saju.B*** *and* ***Mr. R .D Praveenkumar*** *for their Cooperation and support for the preparation of the thesis. I also want express my gratitude to* ***Dr Sunil Sunny*** *for his cooperation during the thesis.*

My thanks also goes to all staff members of the Department of Physics, University of Calicut, for their support throughout the thesis.

I wish to thank ***Mr Sasisekhar****, Kirloskar Theratronics for providing the necessary details of telecobalt machine.*

I wish to thank my wife ***Dr Vijayalekshmi*** *and my beloved Son* ***Govind*** *for being understanding and cooperative during my research.*

Most importantly I want to thank my parents ***Somasekharan Nair*** *and* ***Vasanthakumari,*** *and my family members* ***Lekha, Anilkumar****,* ***Rekha*** *and* ***Saji Kumar*** *for their support and Love showing me through out my life.*

SANTHOSH V.S.

CONTENTS

PAPERS PRESENTED

- Santhosh VS, Saju B. Sushama P, Babu BRS. "Monte Carlo simulation and Beam characteristic studies". Seventeenth National symposium on Radiation Physics (NSRP –17), Indian society of Radiation Physics and the Saha Institute of Nuclear Physics, Kolkata, 2007.

- Sushama P, Santhosh VS, Saju B, Babu BRS. "Dosimetric studies on carcinoma breast treatmets". Seventeenth National symposium on Radiation Physics (NSRP –17), Indian society of Radiation Physics and the Saha Institute of Nuclear Physics, Kolkata, 2007.

INTRODUCTION

The discovery of X Rays by Roentgen in 1895, and Radioactivity by Henry Becquerel in 1896 marked the beginning of many new inventions and branches in physics. The potential of X rays and gamma radiations for the diagnosis and treatment of diseases were realized soon after their discovery. First application of radiation for therapeutic purpose was made in 1896 for the treatment of a breast carcinoma. The first case of cure of malignant disease by radiation was reported in 1899 on a patient with a histologically confirmed squamous cell carcinoma of nose[1]. Introduction of Cobalt-60 isotope machines, design of linear accelerators, advances in quantitative dosimetry and the development of computing techniques and their application to imaging, took the therapeutic applications radiation to newer heights[2]. These developments provided accurate targeting of radiation to the tumor with minimum damage to the healthy tissue surrounding the tumor. New treatment techniques resulted in impressive results in the treatment of prostate cancer, various head and neck cancers, uterine cervix cancers, breast as well as Hodgkin lymphoma[3]. Today it is well recognized that over 40% of cancer treatment results were obtained directly from the use of ionizing radiations.

Commonly used radiations for cancer treatments are X rays and Gamma rays. High-energy electrons, Neutrons, protons, pions etc are also occasionally used for treatment purposes. These radiations can be classified into two main categories -directly ionizing and indirectly ionizing radiations. Directly ionizing radiations are charged particles, such as electrons, protons, etc. They ionize atoms through direct Coulomb interactions with orbital atomic electrons. Indirectly ionizing radiations are neutral particles, such as photons and neutrons, which ionize matter through an intermediate step of first releasing a directly ionizing particle which then ionizes matter through Coulomb interactions.

When a beam of radiation passes through a medium, the energy of the radiation is deposited in the medium. The transfer of energy from a photon beam to a medium takes place in two stages. In the first stage the photon transfers the energy to the medium by primary interactions such as Photoelectric, Compton, pair production or photonuclear disintegration. Through the primary interaction secondary particles like energetic electrons are produced which intern cause further ionization and excitation. High energy photons sometime interact with atomic nucleus to produce nuclear excitations or the emissions of nuclear particles and occasionally radioactive products. Two quantities are defined to quantify this energy deposition – Kerma and Absorbed dose. The quantity KERMA is defined to quantify the average amount of energy transferred from photons to electrons without concern as to what happens after the energy transfer. The high energy electrons move through the medium and transfer some of their kinetic energy to the medium by ionization and excitation (resulting in Absorbed Dose or simply Dose) and loose some of their energy in the form of radiative losses. The transfer of energy and absorption of dose does not take place at the same location because the secondary electrons travel in the medium and deposit energy along their path. Both Absorbed Dose and Kerma express a quantity of energy per unit mass. The difference between the two comes from where this energy is deposited within the medium. For Kerma, it does not matter whether the charged particles slow down inside the volume of interest or not; only the energy transferred to charged particles in the volume of interest is important. For the absorbed dose, on the other hand, only the energy deposited in the medium by the secondary electrons within the volume of interest is considered. The units of both Kerma and absorbed dose are joule per kilogram (J/kg). The special name for the unit of absorbed dose is Gray (Gy) [4].

In case of directly ionizing radiations like protons, electrons and other heavy particles the interaction mechanisms are different. They directly transfer their energy to the medium by processes such as Elastic or in

elastic scattering, capture events with the nucleus, increase or decrease of rest mass or the formation of radioactive products. A quantity CEMA is defined to quantify the energy transfer for directly ionizing radiations.

All living organisms are made up of protoplasm that consists of inorganic and organic compounds dissolved or suspended in water. The smallest unit of protoplasm capable of independent existence is called cell. Cells contain inorganic compounds (water and minerals) as well as organic compounds (proteins, carbohydrates, nucleic acids, lipids). Two Important structures of a cell are the cytoplasm, which supports all metabolic functions within the cell, and the nucleus, which contains the genetic information (DNA). A group of cells that together perform one or more functions is referred to as tissue. A group of tissues that together perform one or more functions is called an organ. An organism is a group of organs. Normally cells propagate through cell division in a controlled and coordinated way by the DNA molecule. Sometimes an uncontrolled or uncoordinated cell growth happens inside the body and this condition is termed as cancer.

When cells are exposed to ionizing radiation, energy is deposited in the cell as a result of the interaction between radiation and atoms of the cells. This energy deposition results the breakage of chemical bonds between the molecules that constitute the cells, causing biological effects. The biological effects of radiation result mainly from damage to the DNA, which is the most critical target within the cell. However, there are also other sites in the cell which, when damaged, may lead to cell death. The damage to the cell occurs by two ways such as direct or indirect action. In *direct* action the radiation interacts directly with the critical target in the cell. The atoms of the target itself may be ionized or excited by the energy deposition leading to the chain of physical and chemical events that eventually produce the biological damage. In *indirect action* the radiation interacts with other molecules and atoms (mainly water, since 80% of a cell is composed of water) within the cell to produce highly reactive free radicals. The free

radicals break the chemical bonds in the target molecules and produce chemical changes that lead to biological damage. About two thirds of the biological damage by radiations such as x-rays or electrons, is due to *indirect* action. The biological effects caused by the radiation can be related to energy deposition by observing the number of cells surviving after irradiation. Cell survival as a function of radiation dose is graphically represented by plotting the surviving fraction on a logarithmic scale on the ordinate against dose on a linear scale on the abscissa. These graphs are called cell survival curves.

When radiation is delivered to the tumor it can cause biological damages to the normal tissues surrounding the tumor also. Normal and tumor tissues have their own radiobiological properties and biological parameters, and the response of normal and tumor tissues depend on the temporal pattern of radiation delivery. To eradicate the tumor cells effectively, enough radiation doses should be given to the tumor without irradiating normal tissues to a dose that will lead to serious complications (morbidity). Such a controlled application of radiation to eradicate tumor cells with minimum damage to surrounding normal tissues can be termed as radiation treatment or radiotherapy.

Radiotherapy procedures fall into two main categories: external beam radiotherapy and Brachytherapy. In external beam radiotherapy the radiation source is at a certain distance away from the patient and the target within the patient is irradiated with an external radiation beam[4]. External beam therapy is also known as Teletherapy. Most of the external beam radiotherapy is carried out with photon beams, some with electron beams, and a very small fraction with particles, such as protons, heavier ions or neutrons. External beam radiotherapy is usually carried out with more than one radiation beam in order to achieve a uniform dose distribution inside the target volume and as low as possible a dose in healthy tissues surrounding the target. The devices used for teletherapy are linear accelerators (Linac),

and cobalt-60 isotope machine (Telecobalt machines). A teletherapy machine consists of two parts. First one is a gantry from which a collimated beam of radiation is emitted and a `treatment couch' on which the patient is positioned. The gantry and couch rotate around a fixed point called isocenter.

Brachytherapy (sometimes referred to as Curie therapy or endocurie therapy) is a term used to describe short distance treatment of cancer with radiations from small and encapsulated radiation sources. Brachytherapy is doing by placing the radiation sources directly into or near the volume to be treated. The dose is then delivered continuously either over a short period of time (temporary implants) or over the lifetime of the source to a complete decay (permanent implants). Commonly used Brachytherapy sources are Iridum-192, Cesiums-137, Cobalt-60, Gold-198 and Iodine-125. With brachytherapy, a high dose can be delivered locally to the tumor with rapid dose fall-off in the surrounding normal tissue. There are two types of Brachytherapy treatments such as (1) Intracavitary, where radiation sources are placed in body cavities close to the tumor volume and (2) Interstitial, where the sources are implanted within the tumor volume[5]. Figure 1.1 Shows the photographs of equipments and systems commonly used for radiation treatment.

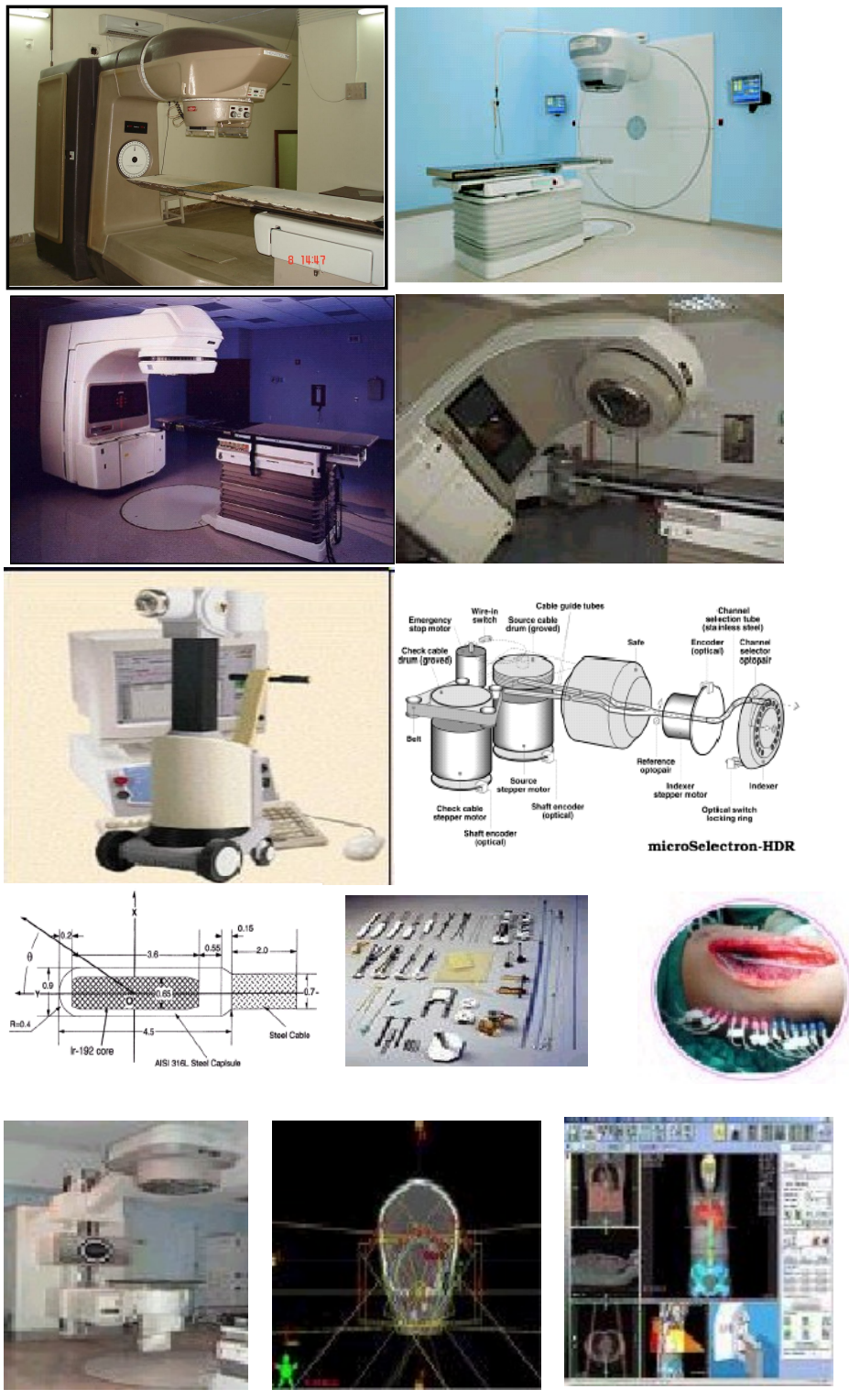

Figure 1.1 Equipments and systems commonly used for radiation treatment

1.2. Treatment planning

Malignant tumors (Cancer) do not have any regular shape, size, type and are usually located or invaded to adjacent critical organs. This complex pattern of tumor makes radiotherapy a complex procedure and involves a number of steps. Treatment planning can be defined as the radiotherapy preparation process in which the procedures and decisions to be made preceding a radiation treatment[6]. The treatment planning procedures involve the selection of the most appropriate type, size, shape and number of radiation fields to achieve a uniform absorbed dose distribution within the tumor. Each step involved in the treatment process introduces a certain level of uncertainty, which can ultimately contribute the success, or failure of the treatment. However accurate Dose distribution within a prescribed accuracy is absolutely necessary to achieve tumor control with minimum normal tissue complications[7-9]. Delivery of radiation dose to the tumor involves many steps and the uncertainty in each step has to be considered in evaluating the final accuracy. Ideally, a comprehensive presentation of all treatment uncertainties should be part of the treatment planning process. An optimization between the required and practically achievable accuracy in dose distribution has to be done before the treatment. Accuracy requirements for radiotherapy treatment should be derived from radiobiological behavior of tumor cells and normal tissues, as well as from clinical evidences [10-15].

The radiobiological response of the tumor as well as the normal tissue can be described by what is referred as dose response curve. Figure 1 .2 shows the dose response curve for normal tissue and tumor cells. The dose response curve has a sigmoid shape, i.e. most of the response occurs within a certain dose interval. The response depends on the type of radiation as well as on the biological characteristics of the tissue. These include the condition of the vascular system, the efficiency of the repair of radiation-induced damages, the delay in growth in different phases of the cell cycle

and the capacity of the resting cells to enter the cell cycle, etc[16]. The normalized dose response gradient "γ", describes how large a change in response probability can be expected for a given relative increase in absorbed dose.

$$\gamma = D\frac{dP}{dD}$$

, Where p denote the response probability for a given dose, D

With increasing dose (D) the normal tissue complication probability and tumor control probability both increases. The curves are slightly steeper for normal tissues than for the tumor. When looking at the steepest portion of dose response curves it can be observed that a 5% change in absorbed dose results 10–30% change in biological response.

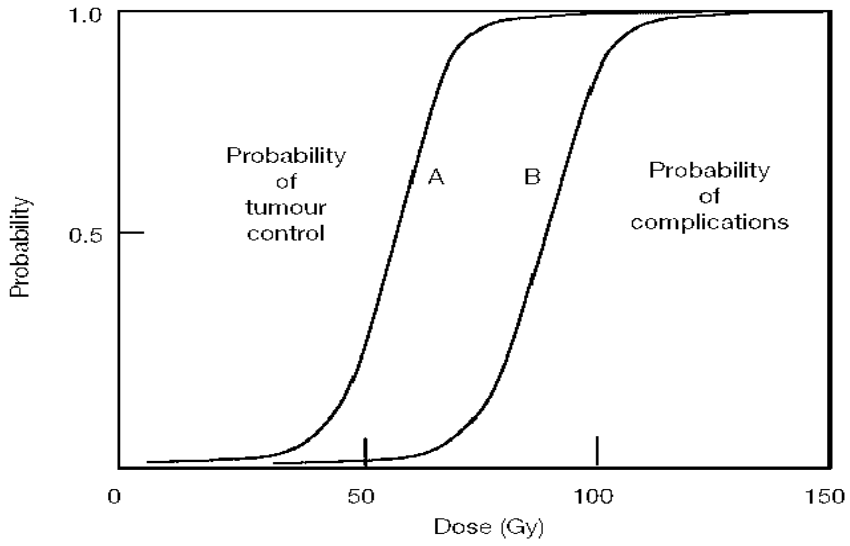

Figure 1.2 Dose response curve for tumor control (cure A) and for normal issue Complication (curve B)

From an extensive review of dose-response data, Brahme *et al*[17] showed that the standard deviation of the mean dose in tumor volume should be at most 3% (one standard deviation) to have control of the

treatment outcome with a 5% tolerance level. This is in agreement with recommendations given by Mijnheer et al [18], based on a review of steepness of dose response Curves observed for normal tissue complications, and other clinical observations.

These clinical/radiobiological observations point to the need that the total absorbed dose to the tumor should be delivered within accuracy of 7-10% of planned absorbed dose. They further concluded that transfer of these data between institutes requires the dose to be known at the dose specification point in the tumor within 7% accuracy, which they equated to 2 S.D. Assuming that this number is equivalent to a confidence level of 95%, the standard deviation in the absorbed dose delivered to the dose specification point must be as low as 2-5%[19-21]. To achieve this accuracy of total absorbed dose to the tumor, the uncertainty in the absorbed dose delivered by the treatment machine to a point (radiation output) under reference conditions should be less than 1.5%(1SD) [22]. The reference conditions are specified by different calibration protocols and will be discussed in the later part of this chapter

The primary task of radiation physics team in radiation treatment planning process is to ensure that a desired amount of radiation dose is delivered to a specified point in the tumor and a desired pattern of radiation (dose distribution) within the patient is achieved. To ensure this, dose measurements within the tumor should be carried out. However, the direct measurement of the radiation on or in the patient is seldom possible and standard measurements must be carried out in tissue equivalent materials. Such tissue equivalent materials are popularly known as phantoms. Phantom is a volume of tissue equivalent materials large enough to provide adequate scatter or constructed to resemble a part of human body, for the purpose of measuring and evaluating dose distributions[23].

Measurements of radiation dose are generally termed as radiation dosimetry. Quantitative measurements of radiation output from a radiation

machine are the first step in clinical dosimetry. The output of a radiotherapy machine is usually stated as the dose rate at a reference depth in a water phantom for a nominal source-surface or source-axis distance (*SSD or SAD*) and a reference field size (often 10x10 cm^2) on the phantom surface or at the isocenter. The output measurements should be carried out to an accuracy better than 1.5 %. In order to achieve this level of accuracy appropriate dosimetry procedures are to be followed using a good quality radiation dosimeter. A dosimeter can be defined as any device that is capable of providing a reading, which is a measure of the average absorbed dose, deposited in the dosimeter's sensitive volume by ionizing radiation. Radiation dosimeters or detectors are designed to perform specific functions such as position sensing, total energy measurement, particle identification. The working of radiation detectors can be summarized as follows:

1. Radiation deposits energy in a detecting medium.
2. Energy is converted into an electrical signal, either directly or indirectly. In the direct conversion process incident radiation ionizes atoms/molecules in absorber, creating mobile charges that are detected. In the indirect conversion dosimeters incident radiation excites atomic or molecular states that decay by emission of light, which in a second step is converted into charge. The electrical charges thus produced result a signal that is proportional to the absorbed dose.
3. The electrical signal is amplified by electronic circuitry. Primary charge is accelerated to sufficient energy for it to liberate additional charge carriers by impact ionization.
4. Pulse shaping.
5. Digitization of signal.

A dosimeter that gives the value of absorbed dose directly is termed as absolute dosimeter. Absolute dosimeter produces a signal from which the dose in its sensitive volume can be determined without requiring calibration

in a known field of radiation (Example calorimeter). The dosimetry procedures using Absolute dosimeters are seldom used in routine applications, as the procedures are cumbersome[24].

In radiotherapy the statement of dosage or machine outputs are made in terms of well-defined unit of absorbed dose. Measured radiation dosage made at various treatment centers throughout the world should be consistent and compatible with each other so that clinical experience can be shared[17]. Although the manufactures of the dosimeters supply an instrument that when used properly gives directly a measurement of dose it is usually necessary to apply correction factors to the reading in order to obtain a correct value of the absorbed dose. The relation between instrument reading and the corresponding value of absorbed dose stated by a standard laboratory is given in terms of a calibration factor. Such dosimeters requiring calibration in a known radiation field are called relative dosimeters. Relative dosimeters are recommended for calibration of radiotherapy machines [24].

Output measurement of a radiation beam is usually carried out by direct measurement of dose or dose rate in water using a relative dosimeter. Several documented procedures were developed for clinical dosimetry. The goal of these clinical dosimetry calibration protocols is to determine the absorbed dose in water delivered by a clinical radiation machine under a specific set of reference conditions[25-27.] A dosimetry protocol provides the formalism and the data to relate the chamber response with the dose established by an international standard laboratory such as IAEA or NIST. The recommended dosimeter by calibration protocols is an ionization chamber because of their simplicity of operation and the ease with which they can be used for obtaining repeated readings with good precision and accuracy[24].

An ionization chamber is an air cavity surrounded by a conductive outer wall having a central collecting electrode [28]. The wall and the collecting electrode are separated with a high quality insulator. Figure 1.3, shows the

working of ionization detector used for the measurement of absorbed dose. When the chamber is exposed to radiation, electrons are liberated within the air cavity. An electrometer is used in conjunction with the ionization chamber to measure the charge produced inside the cavity. If Q is the total charge produced inside the cavity and m_{air} is the mass of air inside the cavity, then absorbed dose can be determined by the following equation;

$$D_{air} = \frac{Q}{m_{air}}\left[\frac{W_{air}}{e}\right] \qquad 1.0$$

Where W_{air}/e is the energy required to produce an ion pair in air per unit Charge. For air, W_{air}/e is 33.97 eV/ion pair or 33.97 J/C.

Dose in air D_{air} so obtained can be converted into dose in water using the Bragg-Gray or Spencer-Attix cavity theories[29]. Schematic diagram of an ionization chamber and measuring electrometer is given in Figure 1.4. An ionization chamber manufactured by CD high-tech, India Ltd, used for calibration of teletherapy machines in our center, is shown in Figure 1. 5.

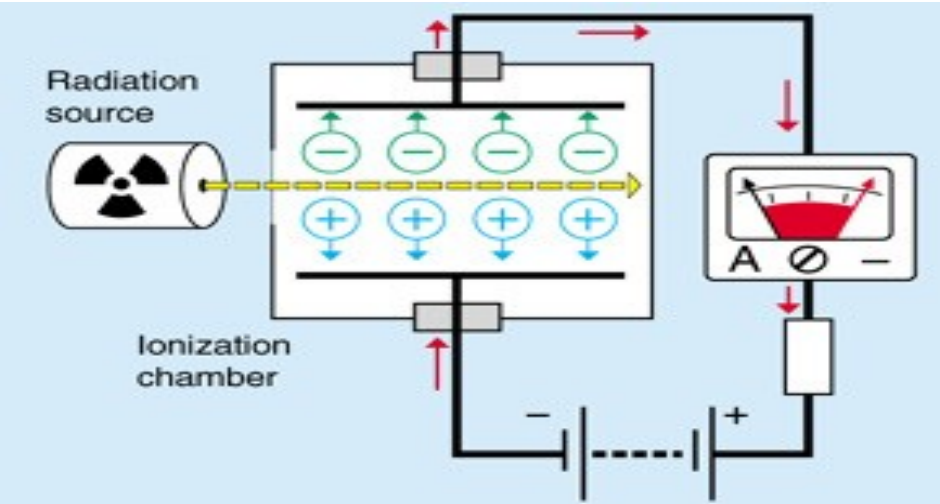

Figure 1.3 Principle of an ionization chamber
(From European Nuclear Society)

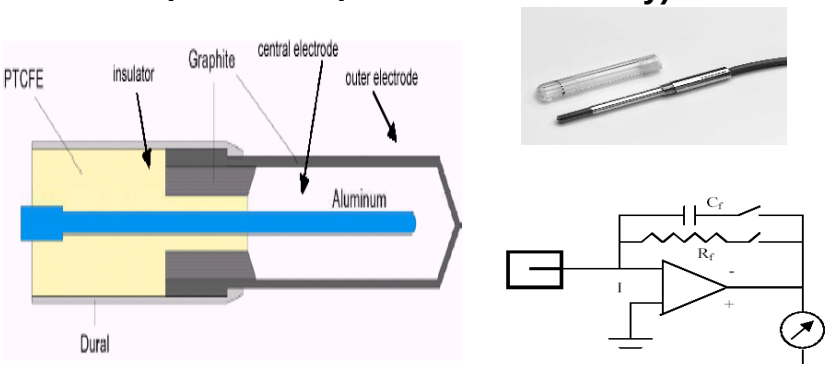

Figure 1.4 Ionization chamber and measuring electrometer

Figure 1. 5 Ionization chamber manufactured by CD high-tech, India

In order to check, whether a desired dose distribution is achieved through out the tumor volume, one needs to calculate the dose over the prescribed volume rather than dose at a reference point. Once the dose at a reference point is established precisely using a standard dosimetric protocol, it is possible to relate dose at other points. This is usually achieved through the use of several dosimetric functions, which link the dose at the reference point in phantom to the dose at any arbitrary point inside the patient. Reference point is usually taken as the depth of Maximum Dose (d_{max}). For ^{60}Co beams reference point is at a depth of 0.5 cm below phantom surface.

1.3 Dosimetric functions

Dosimetric functions are used to link the dose at the reference point in phantom to the dose at any arbitrary point inside the medium. Following are some of the dosimetric functions used for clinical dose calculations. Here the referred medium will be either phantom material or human tissue.

Percentage depth dose (PDD)

Percentage Depth Dose expressed as a percentage, at any depth in a medium is the ratio of the dose at that depth to the dose at a reference depth along the central axis of the beam. Mathematically, the equation for percentage depth dose is:

$$PDD = \frac{D_d}{D_{ref}} \times 100 \qquad 1.1$$

Where D_d is the dose at the arbitrary depth d and D_{ref} is the dose at the reference point, which is on the beam central axis at the depth of maximum dose, d_{max}.

Radiation field and Beam profiles:

Beams used for radiotherapy have various shapes that usually represent a compromise between the actual target shape and the need for simplicity and efficiency in beam shaping. Four general groups of field shapes are used for treatment. They are square, rectangular, circular, and irregular fields. Square and rectangular fields are usually produced with collimators installed in radiotherapy machines. Circular fields are obtained with special collimators attached to the treatment machine while irregular fields are produced with custom-made shielding blocks or with multileaf collimators attached to a treatment machine.

Beam profiles are a representation of the variation of the dose across the field at various depths in the phantom.

Relative dose factors:

Relative dose factor is defined as the ratio of dose at reference depth in a medium for a given field size A to the dose at the same depth for a reference field size A_{ref}. *Reference* field size is usually taken as 10x10 cm^2

Tissue Air Ratio:

Tissue-air ratio (TAR) at any depth in a medium (tissue) is defined as the ratio of dose at that depth in the medium to dose within a small mass of medium in air. Mathematically TAR can be written as:

$$TAR(d, A_d) = \frac{D_d}{D_{air}} \qquad 1.2$$

Where D_d *is* the dose at a depth *d* in the medium, D_{air} is the dose at *d* in a small mass of tissue large enough to produce electronic equilibrium condition, and A_d is the field size defined at depth *d.*

Peak scatter factor:

The total dose delivered at a point in a medium is due to primary and scattered photons. If we are able to prevent the production of scattered photons within the medium, then the dose at d_{max} would equal to the dose delivered by the primary photons only. The ratio of the total dose to the primary dose at d_{max} *is* called the peak scatter factor *(PSF).*

$$PSF = \frac{D_p}{D_T} \qquad 1.3$$

Where D_p and D_T are the total and primary doses at d_{max}, for field size defined at d_{max}. With the aid of *PSF* and other dosimetric functions, such as *PDD* and TAR, the exposure at any other point on the central beam axis in the medium can be calculated.

In short, in order to deliver an accurate radiation dose to the tumor, three important steps are involved. The first step is the establishment of Primary standards of absorbed dose in water. The second step is the establishment of the dose under reference conditions in the therapy beam using an ionization chamber and a calibration protocol. The final step is to establish the dose distribution in individual patient. However, the accuracy of ionization chamber dosimetry is affected by many factors[30-32]. Dosimetric procedure using ionization chambers requires a variety of correction factors such as correction factor for the attenuation and scatter of photons in the walls of the ionization chamber. The inherent errors associated with detector systems and experimental set up can also affect the accuracy of the measured dose. The dosimeter response depends on environmental conditions such as temperature and pressure. Since ionization chamber dosimetry involves a chain of measurements and a variety of correction factors, a dosimetry verification system is highly useful to have confidence in the measured values. Moreover In clinical dosimetry direct measurements of beam characteristics in a patient body are not practically possible, as we cannot introduce detectors inside the human body. Strict ethical conditions

for conducting experiments on human beings also prevent us from such trials. In such situations mathematical modeling and computer simulations are useful for the verification of current dosimetry systems and predicting doses inside the patient where measurements are seldom possible.

Computer Simulations and mathematical modelings are established techniques in scientific research[33, 34]. Mathematical modeling using Monte Carlo methods are the most widely used method for solving many radiation transport problems in nuclear and particle physics[35]. Such simulations have a potential use in clinical radiation dosimetry also[36]. Simulations can be used to obtain the beam reference data necessary for the dose calculations with out doing tedious and time-consuming experiments. Monte Carlo simulations are mathematical technique, which can also be utilized for verification as well as a guiding tool for a variety of experimental methods in medical radiation physics.

Review of the literature:

Petty et al[37] in 1 983 using Monte Carlo method investigated the build up doses from electron contamination of clinical photon beams. The contribution made by contaminating electrons present in a clinical photon beam to the buildup dose in a polystyrene phantom had been calculated and compared with measurements.

Yang et al[38] studied electron contamination in clinical accelerator photon beams using EGS4 based Monte Carlo user code BEAM and MCSIM. The energy spectra of the contaminant electrons are determined for different clinical accelerators. The Monte Carlo calculated dose distributions were compared with measured data and the results showed good agreement (less than 2% or 2 mm) for 6, 10 and 18 MeV photon beams.

Rogers et al[39] (1985) reported calculations of electron contamination in a ^{60}Co beam from an AECL therapy unit using EGS4 code. Their study was limited to broad beam conditions with 35×35 cm^2field sizes and made several approximations owing to low computing time.

Kase et al[40] (1988) determined the primary dose in ^{60}Co gamma beams using a small attenuator and a solid water phantom manufactured by RMI Corporation, Wisconsin with a source to Surface Distance of 80cm.

Nizin et al [41] showed that primary radiation could be determined for field sizes10x10 and 20x20 at depths of 0.5cm, 5cm and 10 cm in water but more improved experimental settings required to minimize experimental uncertainties'.

Udale et al[42] (1992) used EGS 4 Monte Carlo code to study the electron beam parameters for three Philips linear accelerators.

Rogers et al (1994) developed special Monte Carlo code BEAM to simulate radiotherapy treatment machines. Eighteen electron spectra from four commercial accelerators were given in their paper[43].

Bjarngard[44], in 1994 studied the methods to improve the analytical expression used to describe the central axis doses for high energy X ray beams, in particular the component due to phantom scattered photons. They concluded that it is possible to simplify the compilation of central axis doses in an X ray beam by generating the data from two geometric variables (1) the depth *d* and (2) *d/s*, the ratio between depth and side of square field along with other parameters like linear attenuation coefficient.

Demarco et al[45] (1994) used the Monte Carlo code MCNP for thick target Bremstrahlung spectrum calculations to bench mark the Monte Carlo code MCNP against a set of precise measurements taken at the institute for National Measurements Standards in Canada. They investigated the validity of the Monte Carlo code MCNP 4A for radiotherapy treatment planning applications. The MCNP code incorporates a coupled electron and photon transport scheme that allows the user to estimate the photon fluence produced from the primary electron interactions. The integrated and mean energy of each Bremstrahlung spectrum were calculated for Beryllium, Aluminum and Lead targets. They demonstrated that MCNP4A is capable of predicting the integrated Bremstrahlung yield within 6% accuracy with experimental results.

British Journal of Radiology[46] (1996) published a survey of depth doses and related data measured in water phantom. Data were collected from different centers around the world and average values of a specific dosimetric parameter were published. In this supplement PSF, TAR and PDD for various radiation beams were presented. Linear attenuation coefficients for various materials were also presented in this work. These reports are used as a guide for clinical dose calculations. BJR periodically reviews the values. It can be noted that the published values of TAR have changed from values they previously published due to the modified concept of PSF. There are two main concerns regarding PSF and TAR values published in BJR supplement 25. PSF and TAR data were limited only to

photon beams with energies less than or equal to cobalt 60 beams even though PDD values are given for mega voltage X ray beams.

Love et al[47] (1997) compared the Percentage Depth Dose data calculated by two popular Monte Carlo codes EGS4 and MCNP. The geometry used for their simulations consisted of a conical photon beam impinging on a cylindrical water phantom of radius 28.21 cm. The photon beam has a radius 5.542 cm at water surface giving an equivalent area 10×10 cm^2. They used monoenergetic sources approximation for calculating the Percentage Depth Dose for three radiotherapy beams (1.25, 1.9 and 3 MeV equivalent to ^{60}Co, 6 MeV, 10 MeV beams). The calculations of Love agree with experimental results beyond build up region. They concluded that monoenergetic approximation is adequate for central axis dose comparisons.

Demarco et al[48] in 1998 developed a CT based Monte Carlo simulation tool for dosimetry planning and analysis and compared the dose distribution generated by MCNP Monte Carlo code with that generated by a conventional treatment planning system (TPS). Demarco suggested that MCNP4A is suitable for photon based radiotherapy calculations due to its specialized lattice geometry package and versatile source structure. They concluded that Monte Carlo Method could serve as an analysis tool for retrospective clinical comparison and conventional algorithm development. They also pointed out the need for more benchmarking experiments, for the routine use of Monte Carlo method in clinical applications.

Hubbell et al[49] (1998) reviewed the photon interaction cross-sections data in the medical and biological context. The probability of a photon of a given energy E undergoing absorption or scattering when traversing a medium can be expressed in terms of linear attenuation coefficients (μ). Since μ is dependent of density (ρ), the attenuation probability is usually tabulated as a function of mass attenuation coefficient μ/ ρ in which the dependence on the density has been removed. This review includes the

selective history of measurements and theory relating to μ/ ρ. Attenuation tables developed by Hubbell and the updated values are available from the computer programme XCOM.

Difillippo et al[50] (1998) published an article about Forward and adjoint methods for radiotherapy planning. They studied the feasibility of sensitivity theory developed for nuclear applications to radiotherapy treatment planning. They implemented forward and adjoint mathematical approaches to calculate the sensitivities of dose distributions in a mathematical phantom. The potential efficiency and strength of forwarded and adjoint methods of dose calculations using state of art radiation transport methods were demonstrated in this work. They use MCNP code that offers the possibility of tagging the tallies according to user-supplied criteria. This powerful capability of MCNP code makes it possible to obtain all information in one run. They concluded that, the sensitivity of dose with position, angular distribution intensity and spectra of radiation source could be calculated efficiently with Monte Carlo Methods. They argue that better optimization of radiotherapy planning is possible with Monte Carlo Methods rather than using trial and error methods.

Ulanovsky et al[51] (1998) suggested a modification to ORNL phantom in simulation of the response of thyroid detectors. They used MCNP code with age specific ORNL phantom series to simulate the transport of photons within the human body.

Mora et al[52] (1999) used BEAM Monte Carlo code to simulate the ^{60}Co beam from an Eldorado-6 Telecobalt unit. They realistically modeled the source capsule and source housing and collimator assembly and observed that the output factor of the telecobalt machine depends on scattered photons from the fixed and adjustable collimator. Because of large computing time they split the calculations in to three steps. In the first step cobalt source and primary collimator were included. The data for the particle reaching the scoring plane before the outer collimator are stored in a

separate compressed phase space file. This large file is then used for the next part of simulation. The second part includes the passage of the particle through the adjustable collimator and the air medium above the surface plane of the phantom. In the third step the phase space files for different field sizes are reused as an input file for dose calculations. In order to improve the efficiency they uses different cut off energies for particle transport. They also used some of the variance reduction techniques such as range rejection of electrons to improve the efficiency of calculation. The electron and photon transport algorithms used by Mora et al are different from that used in our work.

Wung et al[53] (1999) experimentally verified the Monte Carlo based calculation in various homogeneous phantoms .The phantom geometries include simple layered slabs, a simulated bone column, a simulated missing layer hemisphere and an Anderson anthropomorphic phantom. They used EGS4 Monte Carlo code for their work. They validated the accuracy of Monte Carlo methods for clinical applications and conclude that long computing time is required to achieve reasonable accuracy. Monte Carlo method can be used as benchmark against other dose calculation methods and also to replace measurements when the measurement is difficult to carryout. They pointed out that to implement Monte Carlo Method for routine treatment planning more and more studies required.

Lewis et al [54] (1999) developed an MCNP based model of a linear accelerator beam. They used MCNP code for simulating major components of the Linear accelerator .The model was initially used to generate the energy distribution and angular distribution of the X ray beam for the Philips Linear accelerator in a plane beneath the flattening filter. The data was subsequently used as a source of X rays at the target positions. They concluded that the technique may be used to calculate energy spectra of any linear accelerator with acceptable results in a reasonable run time and has further advantage of that it is far simple to construct complex geometries

compared with EGS4 code system. The use of MCNP on a personal computer should allow a wider use of beam transport modeling in radiotherapy physics applications especially routine quality control tool for linear accelerators and treatment planning systems.

Sheik et al[55] (2000) compared the measured and Monte Carlo simulated dose distributions from the NRC Linac using BEAM Monte Carlo code system. A detailed geometry of LINAC is included in their simulation for two energies 10 and 20 MeV. At both the energies the calculated and measured PDD values are in good agreement (within 1%). The calculated and measured values show some discrepancies in the build up regions. They concluded that the knowledge of exact geometry of collimators is necessary to correlate measured and simulated behavior in the penumbral region and further pointed out that BEAM code is capable of very accurately simulating the photon beams from medical Linacs. However the accuracy depends on information about both the accelerator head and incident electron beam.

Biju et al[56] (2000) developed a mathematical phantom of an Indian male, similar to that of a MIRD phantom. The dimensions of the organs in the MIRD specification were altered to arrive at a phantom representing an average Indian male. Biju used MCNP code version 3.1 to determine the dose received during the diagnostic X ray procedures. The study focused only on diagnostic X rays. Their results show that normalized dose is higher for an average Indian adult than that for the MIRD phantom because of the smaller build of an average Indian.

Rogers [57] (2001) reviewed the applications of Monte Carlo techniques for primary standards of Ionizing Radiation and for Dosimetry protocols. Their major emphasis is on how Monte Carlo technique of electron and photon transport can be applied in radiation dosimetry and primary standards for air Kerma.

Reynaert et al [58] (2002) conducted a detailed study of electron transport in MCNP code and pointed out that that care should be taken when modeling beta-emitting isotopes due to possible errors in electron transport. When care is taken it is possible to obtain correct results that are in agreement with other Monte Carlo code.

Alesia et al[59] (2002) calculated the energy response of a 4π gamma reentrant well-pressurized ionization chamber using MCNP Monte Carlo code. They reported that the flexibility of the geometry description package used in MCNP code makes it easy to model complex ionization chambers. Session et al (2002) compare the point and average organ doses within an anthromorphic physical phantom and computational model of a newborn patient The MCNP code was used for computational modeling and Physical measurements were carried out using MOSFET detectors. The tabulated results of Session can be used as a reference data for estimating the internal organ doses during X ray investigations.

Rnutbrown et al[60] (2002) revaluate the absorbed dose in graphite to water conversion factors for high energy photon beams using Monte Carlo methods. Damilakis et al[61] (2002) estimated the normalized fetus dose for abdominal radiographic examination using MCNP code. The computational approach was verified by comparison with dose data obtained in anthromorphic phantoms using TLD dosimetry. Their results showed that accurate estimation of fetus dose due to abdominal conventional x-ray examination can be made using the dose data provided by them.

Bohm et al [62] (2002) conducted the brachytherapy dosimetry of ^{125}I and ^{103}Pd using an updated library for the MCNP Monte Carlo code. They compared the PDD values obtained from simulation to the values published in BJR Supplement 25.

Tiemori Schani et al[63] (2003) used Monte Carlo code MCNP4C together with ENDEF/BV1 cross section data to simulate a telecobalt machine.

Brain Wang et al[64] (2004) applied the Adjoint Monte Carlo methods to study the dose distribution in a 3D anatomical model called VIP man model constructed from visible human images. They demonstrated the feasibility of the Adjoint Monte Carlo in selecting the beam direction as part of treatment planning based on the anatomical information in a 3D and realistic patient anatomy. They further, in 2005, investigated the issues related to the use of MCNP code for an extremely large voxels volume. They compared different tallies for organ dose calculations and conclude that although there have been many improvements in computer speed and tallies in MCNP the current versions of MCNP code remains unable to handle whole VIP man model at the original voxels size. They also stressed the need for more and more investigations to streamline the use of MCNP Monte Carlo code for routine radiation treatment planning[65].

Rogers et al[66] studied the use of Monte Carlo methods for routine clinical treatment planning. They argued that even though Monte Carlo techniques represent the ultimate answer to the problem of accurate dose calculation the speed of calculation is still the issue. A second issue is the accuracy of the calculation. An accurate specification or the modeling of the clinical beam (including patient specific shaping devices) is essential for the overall calculation to be more accurate. They concluded that implementation of Monte Carlo code for routine clinical treatment planning require the development of various standard tools for comparing various approaches and for assessing the speed of the calculation in a meaning full way.

Considering all the above, it may be noted that Monte Carlo modeling represents an answer to the problem of accurate dose calculation. At the same time above investigations stressed the need for more and more works on clinical application for the efficient use of this powerful and novel mathematical method for the cure of cancer patients. With this objective we have investigate the feasibility of Monte Carlo methods for mathematical

modeling in radiotherapy. This thesis focuses on the mathematical modeling of three radiation transport situations encountered in radiotherapy.

Motivation and objectives of present work

Cancer is the world's most common killer disease keeping Cardiac disease behind. World Health Organization (WHO) estimated 2.5 million deaths in 1997 and 6 million in 2003 and currently10 million people are diagnosed of cancer every year. By the year 2020 WHO estimates over 15 million new cancer patients of which 10% will be from India. Along with other chronic non-communicable diseases, cancer is gaining increasing importance as a public health issue and affects approximately 0.8 million people every year in India[67]. World health Organization in the year 2000 conducted a study evaluating the Disease Adjusted Life Years (DALY) lost from various chronic non-communicable diseases. DALY was used as a combined measure of the years of life lost due to premature mortality in the population and the years of life lost due to disability. The findings of this study showed that, in India, the 8.7 million Disease Adjusted Life Years lost from cancer, was second only to ischemic heart disease (14 million) and more than stroke (6 million) and diabetes (2 million) [68].

There are three major treatment methods such as Radiotherapy, Surgery and Chemotherapy for the management of cancer of which radiotherapy is required for 50% to 70% of cases. As per recent estimates one million cancer patients in India required radiation treatment. Radiation treatment is being carried out in India using Telecobalt machines and Linear accelerators. Around 300 tele cobalt machines are used for radiotherapy in India. An estimated 1500 additional machines are required in future. Cobalt machines are the main workhorses for radiotherapy in our set ups because of their relatively lower costs, simplicity of design, and ease of operation. Cobalt machines produces a predictable output that is totally unaffected by temperature and humidity and other external conditions. Large penumbra and low out put are the main drawbacks of telecobalt machines.

The use of mega voltage radiation beams reduces the skin reaction during treatment. Even though ^{60}Co machines were the first truly practical mega voltage therapy machines, sometimes it is observed that unacceptable skin reaction observed when patients are treated with ^{60}Co beams. These reactions are more prevalent for larger field sizes. The reason for this reaction will be the higher surface dose. Conventional treatment planning systems used to calculate patient doses will not predict accurately the surface doses. Treatment planning systems predict dose accurately only beyond d_{max}. Another interesting fact observed in literature is the reported values of linear attenuation coefficients for cobalt 60 beams. The linear attenuation coefficients published in BJR and NIST show 4% difference[69, 70]. The difference in reported value of linear attenuation coefficients is due to the difference between energy of cobalt beams used for calculation. BJR estimated the linear attenuation coefficient by doing measurements in a telecobalt machine.

In addition to the above facts many modern features of Linacs, such as Multileaf collimators, dynamic wedges could also be installed on modern cobalt-60 machines to allow, at a lower cost, a similar sophistication in treatment as Linacs do.

Considering these facts regarding telecobalt beams we feel that it is necessary to have a thorough understanding about the radiation beam characteristics of a telecobalt machine. With this objective a detailed modeling of telecobalt machine is under taken. In the present work it is proposed to develop a mathematical model of the telecobalt machine and established the characteristics of radiation beams from the telecobalt machines using Monte Carlo methods and the determination of dose calculation parameters of this virtual machine. The study consists of two parts. First part is the determination of primary spectrum of photons emitting from a telecobalt machine. This information is very vital in the context of separating the total photon fluence in to primary and scattered components.

The energy spectrum can be used for further simulations if one wants to simulate the cobalt machine. The second part consists of obtaining dosimetric functions of the simulated telecobalt machine useful for patient dose calculations and comparing with actual measurements.

The invention and use of the ^{60}Co teletherapy unit provided tremendous results in cancer treatment, and placed the cobalt unit into the forefront of radiotherapy for a number of years. Though ^{60}Co machines were widely used, it became necessary to look for sources with greater energy and flexibilities. In this regard, the potential for the use of Linear accelerators in radiation therapy has become apparent in 1950s and the first clinical Linac was installed in 1950s at the Hammersmith Hospital in London, U.K[72]. During subsequent years, the Linac became the most widely used radiation source in modern radiotherapy in developed countries.

Various types of Linacs are also available in our country for the clinical use. The designs of these Linacs are different for different manufactures. This difference in design influences the spectral distributions of photons coming from the Linac. Even though accelerators are specified in terms of their nominal energy the emerging spectral behavior of the photons are significantly different. The difference in spectrum affects the central axis Depth Dose characteristics of the beams. One way to characterize the Central axis dose distribution is to normalize the dose at depth with respect to a reference depth and this quantity is known as Percentage Depth Dose (PDD). Percentage depth Dose tables are used for calculating dose within the patient. Linear accelerator is a delicate machine and the stability of the machine should be ensured before treatment. The output of the machine is strongly affecting the dose distribution within the patient and therefore the outcome of the cancer therapy. Hence it is absolutely necessary to establish a beam quality specifier to periodically check the stability of the accelerator. PDD at 10 cm depth can be used as a beam quality specifier for accelerator beams to check the output stability of a linear accelerator[46.]

In the present work we examine the feasibility of Monte Carlo method for the mathematical modeling and determination of Central Axis Depth dose characteristics and beam quality specifiers of different linear accelerator beams used in our country.

Human body consists of bones and tissues with different physical and radiological properties. Air cavities such as oral cavity, sinuses and lung may also exist in varying thickness. Standard isodose tables and charts for dose estimation are prepared by assuming human body a homogeneous medium of unit density. But the inhomogeineities present in the human body can disturb the dose distribution. In order to achieve better tumor control it is essential to perform the dose calculations by considering these in homogeneities also. Accurate calculation necessitates knowledge of thickness and composition of inhomogeineities and exact behavior of the incident radiation through the inhomogeineities.

The interface effects in the presence of inhomogeineities are a common dosimetric problem encountered in routine treatment planning process. Treatment-planning systems, used to estimate dose distribution for treatment planning is based on a set of measured data along with advanced dose calculation algorithms. Measurement of dose at the interface between two media is impossible and Conventional treatment planning systems cannot exactly predict the characteristics of dose distributions under the perturbation of inhomogeneities[73, 74]. In the present work we mathematically modeled various tissue inhomogeineities using Monte Carlo methods and studied the effects of inhomogeineities in the depth dose distributions.

The overall objectives of the present investigations can be summarized as follows:

1. Mathematical Modeling of a Telecobalt machine using Monte Carlo method and computation of the Dosimetric parameters of this virtual machine.

2. Modeling and study of depth dose characteristics of high energy Linear accelerator beams using Monte Carlo methods.

3. Mathematical modeling of homogeneous and heterogeneous human tissues using Monte Carlo method and the study of the effect of inhomogenieties on central axis depth dose characteristics.

1.7. Overview of the thesis:

Following the introductory chapter, Chapter 2 introduces the mathematical description of the radiation transport problems. The radiation transport can be represented by a continuous Boltzmann transport equation .The solutions to the Boltzmann transport equations can be determined either by deterministic methods or Monte Carlo methods. Monte Carlo methods and their advantageous over other methods are discussed in this chapter. An overview of the Monte Carlo code used in the present work is given in this chapter.

Chapter 3 deals with the mathematical modeling of telecobalt machine commonly used for cancer treatment in India. Maximum effort has been taken to have a realistic model of the machine. Various dose calculation parameters of the machine are evaluated and compared with the experimental results and presented in this chapter.

Chapter 4 deals with the mathematical modeling and study of dosimetric parameters of high-energy X ray beams from linear accelerators, using Monte Carlo methods. Simulated results are compared with experimental results.

Chapter 5 discusses the modeling of human tissues using Monte Carlo methods, and the observed variations of central axis depth dose characteristics of clinical radiation beams in the presence of inhomogeneties present in human body were presented.

A brief summary and overall Conclusions of the present investigations are given in chapter 6. Representative Monte Carlo modeling outputs of the present investigations are given in appendix I, II, III and IV.

CHAPTER 2

MATHEMATICAL ASPECTS OF THE RADIATION TRANSPORT AND MONTE CARLO METHODS

Mathematical modeling of radiation transport phenomena through a medium involves the study of radiation beam penetrating through the medium and surrounding air and the determination of photon fluence or energy deposited at different points in the medium. For an analysis of radiation transport process both the radiation and the background can be considered as particles. We can refer these particles as radiation particles and background particles. Further, we assume that the background particles can be set in rapid motion as a result of interactions with radiation particles, thereby becoming radiation particles themselves.

When a photon beam is incident upon a medium secondary particles are generated in the medium. A parameter Yield (Y) is defined to quantify this secondary particle production. Yield is crucial parameter as far as energy deposition is concerned. Yield is a function of both angle and particle energy and is usually expressed in terms of particles per unit solid angle at the point of interest and is commonly normalized to the number of incident particles. Yield can be theoretically obtained if we know the rate of production of secondary particles.

The rate of production of secondary particles and their energy spectra can be obtained from the cross-section of that particular collision reaction. Yield can be directly obtained from the differential reaction cross-section

$$\frac{d\sigma_{(\theta,E)}}{d\Omega},$$

Where $\sigma_{(\theta,E)}$ is the reaction cross section as a function of incident particle energy (E) and the polar angle(θ), relative to the direction of incident

particle. Ω is the solid angle in which the secondary particles are produced. Yield could be obtained from an integration of this cross section over θ and E as these quantities varies while the incident particle passes through the medium.

In clinical radiation transport modeling two quantities are required to determine the absorbed dose at a point (r, θ). First quantity is the particle fluence, given by the total number of particles per cm ^{2} per incident particle. Second quantity is called differential fluence $d\Phi_{(\theta,E)}/dE$ given by the total number of particles per cm^2 per Mev per incident particle. These quantities can be obtained once the details of angular distribution of secondary particle yield ($dY_{(\theta)}/d\Omega$) and angular dependence of the emitted particle energy spectrum $\frac{d^2Y(\theta,E)}{dEd\Omega}$ are determined.

Total fluence at a given distance r at a specified angle θ is given by

$$\Phi(\theta) = \frac{1}{r^2}\frac{dY(\theta)}{d\Omega} \qquad 2.1$$

And the differential fluence is given by

$$\frac{d\Phi(E,\theta)}{dE} = \frac{1}{r^2}\frac{d^2Y(E,\theta)}{dEd\Omega} \qquad 2.2$$

Given the fact that the secondary as well as primary particles can create radiation fields it is quit obvious that radiation field at a point is a mixture of stray and direct radiation, and it will be a function of energy, direction and particle type. We can assign magnitude to this multidimensional quantity by integrating over energy and direction of the product of angular flux and an appropriate conversion factor. If the selected conversion factor is flux to dose conversion factor the result of this integration will be the absorbed dose D at that particular location.

This relation can be written as;

$$D(x,t) = \sum \oint_{4\pi} d\vec{\Omega} \int_0^{\infty} dE f_i(x, E, \vec{\Omega}, t) P_i(E) \qquad 2.4$$

Where the summation index "*i* "is over various particle types, Ω is the direction vector of particle, *x* is the coordinate vector of the point in space where dose is to be calculated and E, *t* and P *(E)* are particle energy, time and a conversion factor respectively.

The factor $f_i(x, E, \Omega, t)$ is called angular flux which is defined as the number of particles of type '*i*' per unit area per unit energy per unit solid angle per unit time at location *x* with an energy *E* at time t and traveling in a direction Ω.

The angular flux can be related to the flux density fluence and energy spectrum as follows

$$\phi_i(\bar{x}, t) = \sum \oint_{4\pi} d\vec{\Omega} \int_0^{\infty} dE f_i(\bar{x}, E, \vec{\Omega}, t) \qquad 2.5$$

The angular flux, $f_i(x, E, \Omega, t)$ is connected to the fluence $\Phi_i(x)$ by integrating over the intervening period of time (t_i *to* t_f),

$$\Phi_i(\vec{x}) = \oint_{4\pi} d\vec{\Omega} \int_0^{\infty} dE \int_{t_i}^{t_f} dt\, f_i(\vec{x}, E., \vec{\Omega}, t) \qquad 2.6$$

and the energy spectrum at point x at time *t* can be written as,

$$\phi_i(x, t, E) = \oint_{4\pi} d\Omega f_i(x, E., \Omega, t) \qquad 2.7$$

The angular flux f_i can be obtained by solving the stationary form of Boltzmann transport equation for radiation transport for each particle type as a function of position and time.

2.1 Boltzmann transport equation for radiation transport:

The Boltzmann equation represents a mathematical statement of all processes that the particles of various types, including photons that comprise the radiation field can undergo. It is an integral-differential equation describing the behavior of a dilute ensemble of corpuscles. This equation is a continuity equation of the angular flux, f_i, in phase space that is made up of the three space coordinates of Euclidian geometry, the three corresponding direction cosines, the kinetic energy, and the time. Boltzmann equation for radiation transport can be derived as follows.

Radiation Density in a volume of phase space may change in five ways. They are (1) *Uniform translation* where the spatial coordinates change, but the energy- angle coordinates remain unchanged, (2) *Collisions* as a result of which the energy-angle coordinates change, but the spatial coordinates remain unchanged, or the particle may be absorbed and disappear altogether (3) *Continuous slowing down,* in which uniform translation is combined with continuous energy loss (4) *Decay;* where particles are changed through radioactive transmutation into particles of another kind; and (5) *Introduction,* involving the direct emission of a particle from the source into the volume of phase space of interest.

An equation can be framed by combining these five elements as:

$$\tilde{B}_i f_i(x, E, \Omega, t) = Q_{ij} + Y_{ij} \qquad 2.8$$

where $\tilde{B}_i$ is the mixed differential and integral Boltzmann operator for particle of type i , given by

$$\tilde{B}_i = \vec{\Omega}\nabla + \sigma_i + d_i - \left\{\frac{\int dE}{\int E dE}\right\} S_i \qquad 2.9$$

and

$$Q_{ij} = \sum_j \oint_{4\pi} d\vec{\Omega}' \int_0^{E_{\max}} dE_B \sigma_{ij}(E_B \to E, \vec{\Omega}' \to \vec{\Omega}) f_j(\vec{x}, E, \vec{\Omega}', t) \qquad 2.10$$

and

$$d_i = \frac{\sqrt{1-\beta_i^2}}{\tau_{i\beta_i} c} \qquad 2.11$$

In the equations 2.8

Yij is the number of particles of type *i* introduced by a source per unit area, time, energy, and solid angle;

σ_i is the absorption cross section for particles of type *i*. To be dimensionally correct, this is actually the *macroscopic* cross section or linear absorption coefficient $\mu = N\sigma$

d_i is the decay probability per unit flight path of radioactive particles (such as muons or pions) of type *i*

S_i is the stopping power for charged particles of type *i* (assumed to be zero for uncharged particles);

Qij is the "scattering-down" integral, the production rate of particles of type *i* with a direction $\vec{\Omega}$, an energy *E* at a location x , by collisions with nuclei or decay of *j*-type particles having a direction $\vec{\Omega}'$ at a higher energy E_B

σ_{ij} *is* the doubly differential inclusive cross section for the production of type-*i* particles with energy *E* and a direction $\vec{\Omega}$from nuclear collisions or decay of type-*j* particles with a direction *EB* and a direction $\vec{\Omega}'$ and β_i is the velocity of a particle of type *i* divided by the speed of light *c* ,and τ_i is the mean life of a radioactive particle of type *i* in the rest frame.

This equation is quite difficult to solve in general and special techniques have been devised to yield useful results. There are two classes of computational techniques that are used to solve the Boltzmann transport

equations. They are energy balance deterministic methods and those based on particle-following stochastic methods. In the first class, namely deterministic methods, the transport equation is discretized using a variety of methods and then solved directly or iteratively. Different types of discretization give rise to different deterministic methods, such as discrete ordinates (SN), spherical harmonics (PN), collision probabilities, nodal methods, and others.

The second class of techniques, Monte Carlo methods, is a statistical simulation technique. Statistical simulation is defined in quite general terms to be any method that utilizes sequences of random numbers to perform the simulation. This method is also known as random walk method. Deterministic methods solve the transport equation for the average particle behavior. By contrast Monte Carlo method does not solve an explicit equation but rather obtains answers by simulating individual particle and recording some aspects of their average behavior. The average behavior of particles in the physical system is then inferred from the average behavior of the simulated particles. No transport equation need ever be written to solve a transport problem by Monte Carlo method and the only requirement is that the physical (or mathematical) system be described by a probability density function that describes the probability density of particles in phase space. This equation turns out to be the same as the relevant transport equation. Once the probability density functions (PDF) are known, the Monte Carlo simulation can proceed by random sampling from the PDF's. Separate probabilistic events that compose the entire process are simulated sequentially by constructing a series of particle trajectories, each segment of which is chosen at random from a distribution of applicable processes. Random numbers between 0 and 1 are selected to determine what and where an interaction takes place based on the physics rules of interaction of radiation with matter and transport data probabilities. Many simulations are then performed (multiple trials or histories) and the desired result is taken as an average over the number of observations. The outcome of these random

samplings, or trials, must be accumulated or tallied in an appropriate manner to produce the desired result. The results will then be processed to yield a mean and standard deviation of the quantity of interest.

Algorithms to allow Monte Carlo methods to be implemented efficiently on advanced computer architecture are called Monte Carlo codes. A Typical Monte Carlo code has the following components.

1. A Source program written in FORTRAN, C^{++} or Visual Basic,
2. A set of cross section values. The cross section data are obtained experimentally and theoretically. Eg: ENDEF, Hansen-Rosch and IAEA
3. User Supplied input data. Input data includes Geometry, material, Radiation source details, tally details such as Dose, Flux, Energy Deposition, Spectrum and other relevant parameters availability of random numbers on the unit interval, must be given.

A general-purpose coupled neutron/photon/electron Monte Carlo transport code is used in the present work. The code treats an arbitrary three-dimensional configuration of materials in geometric cells bound by first- and second-degree surfaces and fourth-degree elliptical tori. The code uses continuous -energy nuclear and atomic data libraries[75]. The primary sources of data are evaluated from the Evaluated Nuclear data File system, Evaluated Nuclear data Library from Los Alamos laboratory. The data in the photon interaction table allow the code to account for incoherent and coherent scattering, the possibility of fluorescent emission after photoelectric absorption, absorption in pair production with local emission of annihilation radiation, and Bremsstrahlung. A continuous slowing down model is used for electron transport that includes positrons, k-X-rays, and Bremsstrahlung but does not include external or self-induced fields. Photons and electrons from 1 keV to 1000 MeV can be successfully transported.

For the Monte Carlo modeling the user creates an input file that is subsequently read by the Monte Carlo code. The input file contains information such as:

- The geometry specification
- The description of materials and selection of cross-section evaluations
- The location and characteristics of the neutron, photon, or electron source
- The type of answers or tallies desired
- Any variance reduction techniques used to improve efficiency

Monte Carlo results or tallies are normalized to be per starting particle and are printed in the output accompanied by a second number R, which is the estimated relative error defined to be one estimated standard deviation of the mean divided by the estimated mean. For a well-behaved tally, R will be proportional to $N^{-0.5}$ where N is the number of histories or trials. Thus, to halve R, we must increase the total number of histories fourfold. For a poorly behaved tally, R may increase as the number of histories increases. The estimated relative error can be used to form confidence intervals about the estimated mean, allowing one to make a statement about what the true result is. It is extremely important to note that these confidence statements refer only to the precision of the Monte Carlo calculation itself and not to the accuracy of the result compared to the true physical value. Accuracy of the true physical value depends on the cross section data, modeling details, sampling techniques and approximations, etc., used in a calculation.

The input specifications for a Monte Carlo calculation can be termed as modeling. For the mathematical modeling of radiation transport situation (eg simulation of treatment machine) using Monte Carlo code, steps as specified below are involved.

The first step is the specification of geometry. Using a set of analytical geometrical equations and corresponding coefficients components of the machine are specified. Each component of the machine can be considered as a geometric cell filed with specified materials. These cells are defined by the intersections, unions and compliments of the region bounded by the surfaces. Surfaces are defined by supplying the coefficients to the analytical surface equations.

Specification of materials filling the cells is another important step for the Monte Carlo simulation. For each material a unique identification number will be assigned. The details to be specified are Elemental composition, Density, Cross section data, Atomic Number and Mass Number.

Definition of source is the next step for the simulation. The location, characteristics and type of radiation particles are specified. Different parameters such as initial energy of the radiation, their probabilities are to be specified accordingly. Monte Carlo results represent an average of the contributions from many particles tracked during the course of the simulation. Relative error associated with a simulation is inversely proportional to $\sqrt{N}$, where N is the number of particles tracked. For a given Monte Carlo run the computer time is proportional to the number of particles tracked. The challenge of an efficient Monte Carlo simulation is to minimize the computing time with minimum relative error. Methods for reducing the variance in the estimated solution to reduce the computational time for Monte Carlo simulation are termed as Variance reduction techniques. Different variance reduction techniques are available in the Monte Carlo code to improve the computing efficiency. Particles originating from the source are tracked through out their life till they are completely absorbed or escape from the problem geometry. Probability distributions are randomly sampled using transport data to determine the outcome at each step of its life. Various quantities related to particle transport such as particle current, particle flux or energy deposition could be estimated during simulation. In a

Monte Carlo simulation the user has to specify the parameters of interest. Tally results are obtained from an output file. In addition to the tally results the output file contains tables of standard summary information to get an idea of how the simulation ran. If errors occur during the running of a problem detailed diagnostic prints for debugging are given. Each tally results are printed with its statistical relative error corresponding to one standard deviation. A tally fluctuation chart is also printed to show other statistical parameters such as the tally mean, error, and variance of variance to ensure the efficiency of calculations.

CHAPTER 4
MODELING OF ACCELERATOR BEAMS

High-energy linear accelerators are used for the treatment of cancer. Medical Linear accelerators are designed to have two modes of treatment, such as Photon and Electron modes. In photon mode, photon beams form the accelerators are used to deposit absorbed dose at a depth within a patient at the site of the tumor while in electron mode electrons are used for such a purpose. Electron mode is ideal for treating superficial tumors while photon mode is ideal for deep-seated tumors. In linear accelerators electrons are first produced by an electron gun, which are accelerated to kilo voltage energies and injected into a wave-guide, which receives its power from a magnetron, klystron or microtron. The electrons leaving the wave-guide are roughly monoenergetic with energy in the mega voltage range. They pass through a bending magnet and are directed towards the tumor within the patient. In photon mode mega voltage photons are created when high-energy electrons are stopped in a target. Resulting photons will have a broad energy spectrum. The target is surrounded by a shield of tungsten that serves as a primary collimator of the photon beam[77].

The intensity of Bremsstrahlung photons from a linear accelerator is not uniform and a flattening filter is used to achieve homogeneous intensity over field widths used for treatment. The shapes of the flattening filter are different for different beam energies and strongly influence the beam characteristics of the Linac. Just below the flattening filter, a dual sealed ion chamber or monitor chamber is mounted for rigorous beam control. The monitor chamber actually measures the dose in arbitrary units called “monitor units” (MU). Generally, the sensitivity of the monitor chamber is adjusted such that 1 MU corresponds to a dose of 1 cGy in a phantom under reference conditions.

The linear accelerator including the beam defining system is mounted within a gantry together with electronic and other systems and this can be rotated around a horizontal gantry axis. The beam central axis intersects the gantry axis at a point in space called the isocenter. Usually, the distance between the target and the isocenter is 100 cm. Schematic representation of a Linear accelerator used for radiotherapy is given in Figure 4.1

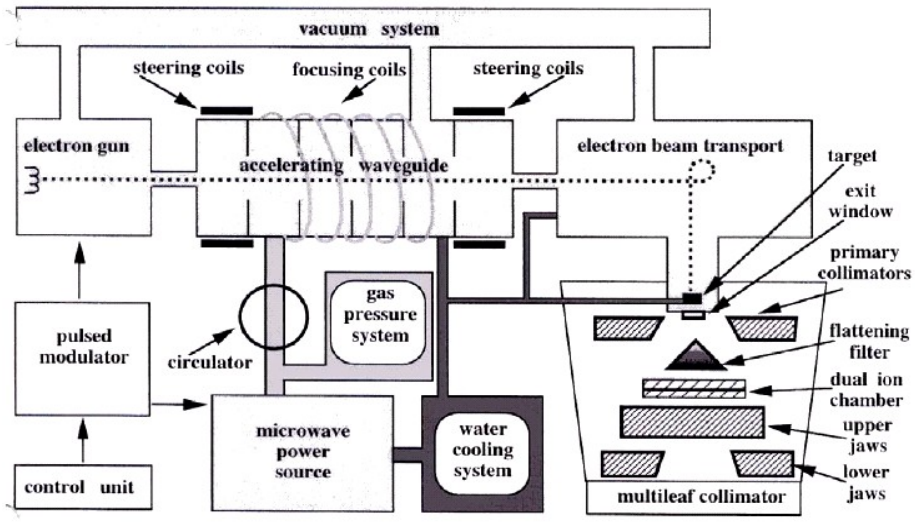

Figure 4.1 Schematic representation of a modern Linear accelerator (Ref: Review of Radiation Oncology Physics , IAEA)

Each photon beam from a Linac in a phantom can be characterized by a three-dimensional dose distribution. A practical representation of this distribution consists of three dosimetric quantities: the depth dose curves, the dose profiles and the output factors. The depth dose curves describe the variation of the central axis dose with depth in a phantom, usually normalized to the dose at d_{max}. The depth dose curve is a function of beam energy, field size and source to surface distance (SSD). The dose profiles give the variation of dose in a phantom perpendicular to the central axis at a specific depth in the phantom. The dose profile is a function of beam energy, field size, SSD and size of the focal spot on the target. The output factor

expresses the dose rate at a point on the central axis in the phantom for a given field in relation to the dose rate in that point for a reference field. The output factor changes with beam energy, SSD and size of the focal spot on the target. Knowledge of these three dosimetric quantities for a treatment beam allows us to determine the dose at any point in the medium.

The spectral distribution of photons produced from the target is the fundamental characteristic of a medial accelerator. The dosimetric quantities used for dose computation are mainly based on the spectral distribution of radiation from the Linac. More over advanced treatment planning systems use the spectral information for dose calculation. The photon spectra from a linear accelerator depend on many factors such as the design of target, collimator systems and flattening filter[24].

Various types of Linacs are available in our country for clinical use. Some provide photons only in the low mega voltage range (4 MeV or 6 MeV) others provide both photons and electrons at various mega voltage energies. A typical high-energy Linac will provide two photon energies (6MeV and 18 MeV) and several electron energies (*e.g*., 6, 9, 12, 16, 22 MeV). The design of Linacs is different for different manufacturers and the difference in design influences the spectral distributions of photons. Accordingly even though accelerators are specified in terms of their nominal energy, the emerging spectral behaviors of the photons are significantly different. The difference in spectrum affects the central axis Depth Dose characteristics of the beams. One way to characterize the Central axis dose distribution of an accelerator is to normalize the dose at a given depth with respect to a reference depth and this quantity is known as Percentage Depth Dose (PDD). Measuring the depth dose variation along the central axis of the beam is a fundamental step to Patient dose calculations. This parameter can also be used as a beam quality specifier for accelerator beams[46]. Beam quality specifiers are used to check the output stability of a linear accelerator before clinical use. The variations in the output of the machine will strongly affect the dose distribution in the patient and therefore the outcome of the therapy.

In this chapter we employ Monte Carlo modeling for the determination of Central Axis Depth dose characteristics and Beam quality specifiers of different linear accelerator beams used in India.

4.2 Materials and Methods:

For the determination of central axis depth dose characteristics we mathematically modeled an experimental setup to determine the Percentage depth dose for various beams from a linear accelerator. The experimental arrangement was modeled using the Monte Carlo methods such that a photon beam from the accelerator is impinging upon the top surface of a phantom. PDD values are then calculated by calculating the energy deposited by these beams at different depths. The phantom is modeled as a square cube with dimension 30 ×30× 30 cm^3 filled with water. Measurement regions having an area 0.5×0.5 cm^2 and depth 20 cm are also included along the central axis of this phantom. The top layers of this region were divided into 1mm for the first 1 cm depth, 2mm thick layers from 1cm to 2cm and 1 cm beyond 2cm depth.

A detailed description of incident radiation beam must be specified for the central axis depth dose characteristics studies using Monte Carlo methods. The incident beam parameters can be obtained by a detailed modeling of the accelerator head. A detailed modeling of accelerator must be performed by starting with an electron beam impinging on the target of the machine being modeled. Every structural details of the accelerator should be specified for such purpose. However the intension of the present study is to establish the depth dose characteristics of the accelerator beams in a water phantom. Therefore a detailed modeling of the accelerator is beyond the scope of the present work. Here we implement a virtual accelerator concept for doing the PDD calculation. The virtual accelerator is a point source from which photon beams are emitted with photon fluence spectral distribution as that of a real accelerator[78]. Fluence spectra are defined as the number of photons per MeV. Sheik and Rogers[79] analyzed the geometry and characteristics of different accelerators available for

clinical use and generated a list of spectral information using EGS4 Monte Carlo code. In the present investigation we use the same spectra generated by Sheik and Rogers, which are available with the National Research Council (NRC) website [80].

In the present work, the photon source was modeled as a point source emitting photons isotropically into the solid angle, which is shaped by a collimating system to give a rectangular field of 10×10 cm^2 at the phantom surface. The source was located at 100 cm from the phantom surface. The collimators are set at a distance of 50 cm from the source. In the present work no collimator or head scatter is taken into account. No flattening filters were included in the model nor was any angular dependence of the energy spectrum. The empty space between the collimators and phantom surface were kept void. These approximations may affect the calculated surface dose due to the omission of air scatter and scattered photons from the collimator. However our aim is to calculated dose variation along the central axis of the beam and these simplifications do not contribute much difference in our simulations results. Percentage Depth Dose was calculated in the phantom at various depths along the central axis of the 10 x 10 cm^2 field by measuring the energy absorbed in different measurement regions. The resultant dose is normalized to the dose determined at depth of $d_{max.}$

We have studied the characteristics of two Accelerators. First one is a dual mode high-energy linear accelerator manufactured and supplied by Electa, Stockholm, Sweden and a Single energy linear accelerator by Varian Associates, USA. Both machines are used for cancer treatment. Electa machine is a dual energy machine capable of producing two photon energies, 6 MeV and 15 MeV. Varian machine is a single energy machine producing 6MeV photons. The actual beam contains a spectrum of energies. Monte Carlo generated photon fluence spectrum for these two machines is obtained from the NRC website. The fluence spectra of these two machines used in this study are listed below (table 4.1)

Electa 6 MeV		*Varian 6 MeV*	
Energy Bin	**Photons/MeV per incident electron**	**Energy Bin**	**Photons/MeV per incident electron**
0.25	1.73E-05	0.25	2.14E-05
0.5	1.00E-04	0.5	1.26E-04
0.75	1.10E-04	0.75	1.31E-04
1	9.52E-05	1	1.14E-04
1.25	8.27E-05	1.25	9.76E-05
1.5	7.21E-05	1.5	8.36E-05
1.75	6.35E-05	1.75	7.25E-05
2	5.57E-05	2	6.23E-05
2.25	4.93E-05	2.25	5.35E-05
2.5	4.37E-05	2.5	4.59E-05
2.75	3.86E-05	2.75	3.95E-05
3	3.45E-05	3	3.65E-05
3.25	3.02E-05	3.25	3.47E-05
3.5	2.70E-05	3.5	2.98E-05
3.75	2.40E-05	3.75	2.61E-05
4	2.10E-05	4	2.25E-05
4.25	1.86E-05	4.25	1.91E-05
4.5	1.64E-05	4.5	1.66E-05
4.75	1.42E-05	4.75	1.14E-05
5	1.21E-05	5	9.04E-06
5.25	1.01E-05	5.25	6.55E-06
5.5	8.17E-06	5.5	4.09E-06
7.25	8.82E-08	5.75	1.40E-06
7.5	1.88E-08	6	4.34E-08
5.75	6.45E-06		
6	4.55E-06		
6.25	3.00E-06		
6.5	1.56E-06		
6.75	7.34E-07		
7	2.94E-07		
7.75	2.77E-09		
8	1.59E-09		

Table 4.1 The fluence spectra of Varian and Electa machines

For all the beams studied in this work we compared our simulated results with the measured PDD values published in British Journal of Radiology[46].

The percentage depth dose values at 10 cm depth (D_{10}) were compared for each machine. The percentage depth dose at 10 cm depth (D_{10}) is a beam quality specifier adopted by many laboratories and manufacturers. This parameter can also be used as an index for machine performance.

4.3 Results and Discussions:

Figure 4.3 shows the Monte Carlo Generated PDD curves for 6 MeV photons with BJR published values superimposed. The calculated results fairly agree with the measured values beyond d_{max}. In the build up region BJR has not published any values because of the large uncertainties associated with surface dose measurements.

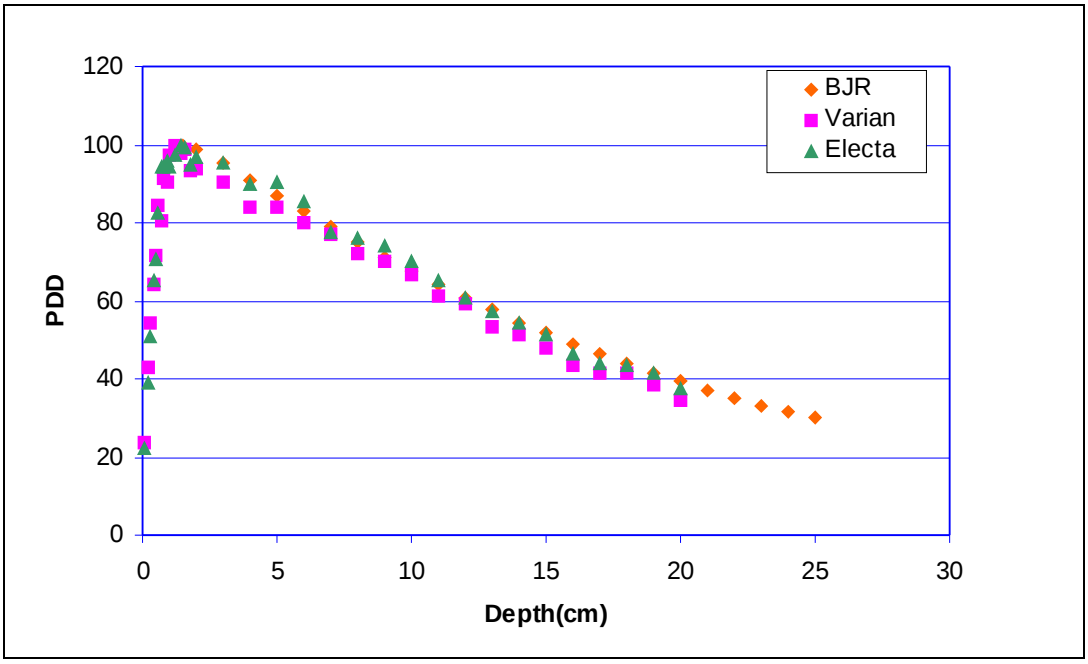

Figure 4.3 Comparison of PDD values for 6MeV accelerators (Electa and Varian)

Table 4.4 shows the results of the depth dose evaluated at 10 cm depth. The beam quality indexes D_{10} for both machines are given in this table. BJR published value for 6MeV photons is 67.5% . For Electa machine the value of D_{10} has a difference of 4 % as compared with in BJR values, while Varian machine shows a variation of only 0.7%. Sheikh et al calculated the D_{10} values using Monte Carlo methods and obtained a value of 66.6 for Varian machine and 68.1 for Electa machines. Our simulation also produce similar results, which clearly indicates that the parameter D_{10} is different for different machines even though the manufacturer specified energies are same (6MeV). The difference in D_{10} is an indication of spectral variation of the two machines.

Machine	Monte Carlo	Measurements
Electa	70.23	67.5
Varian	68.09	68.1

Table 4.4 Values of the Depth Dose in the reference depth 10 cm in eater at SSD 100 cm for 6 MeV photons

For 25 MeV photons the simulated and BJR published values are shown in figure 4.4.The values are generally in agreement with published values. However the simulated values are slightly higher than the representative data published in BJR. This indicates there is slight difference between published PDD values for Electa accelerator. Our study therefore recommends that individual measurements of beam parameters to be carried out before clinical use instead of using reference data directly. PDD at 10 cm depth for Electa accelerator is calculated as 88.35 while BJR published value is 83(deviation of 6%). Our study also indicates that a general beam quality index cannot be used for accelerators. It is therefore necessary for the institutions using the accelerators to independently

establish the beam quality index for routine verification of accelerator stability.

In addition to the high energy beams mentioned above, we have simulated two more intermediate energy beams used for routine patient treatment. Figure 4.5 and Figure 4.6 shows the comparison of Monte Carlo simulated and BJR published values for 10 MeV and 15 MeV Beams.

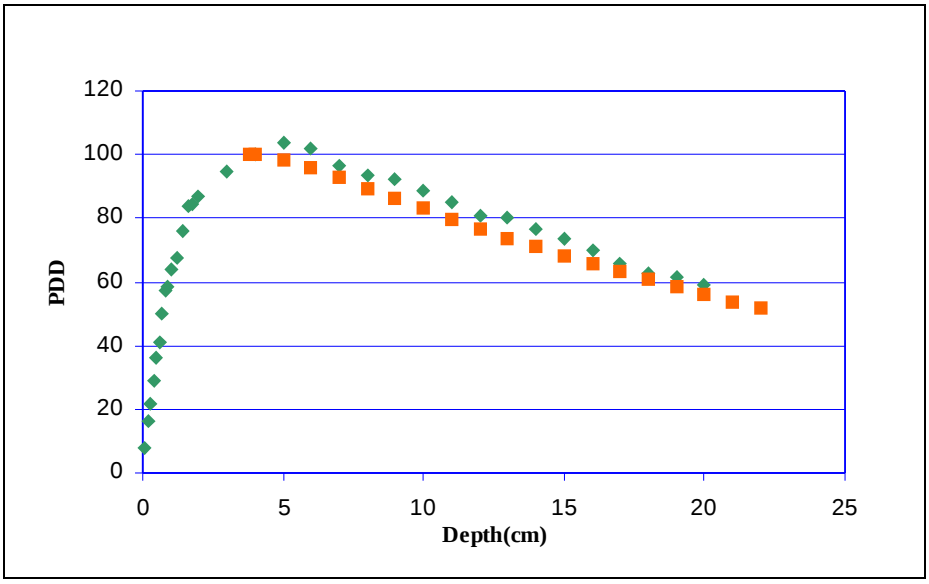

Figure 4.4 Monte Carlo simulated and Published PDD values for 25 MeV photons from an Electa Machine

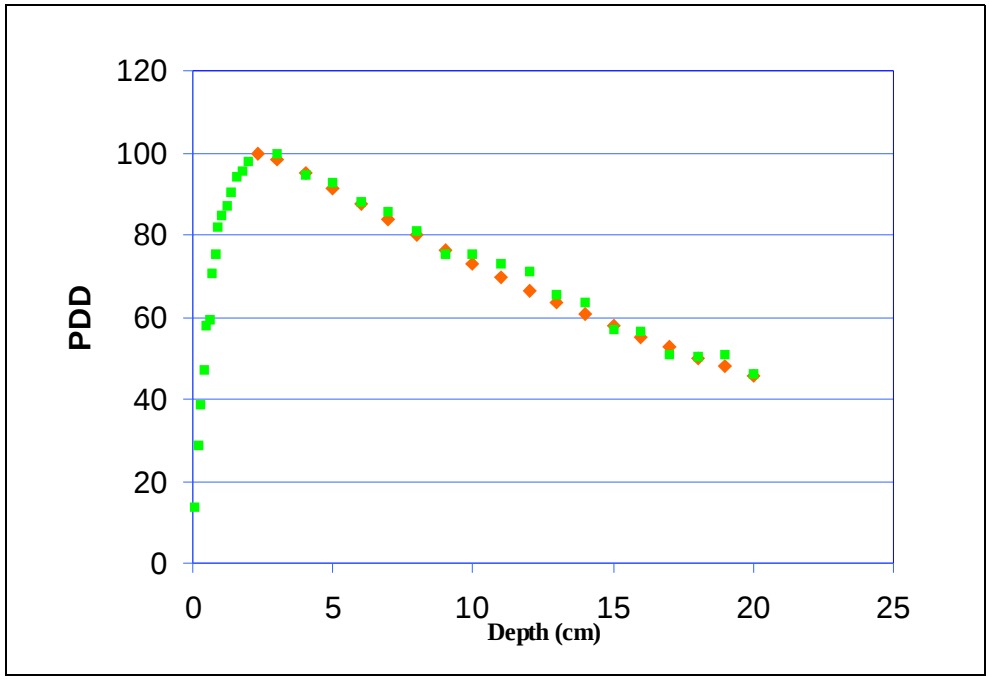

Figure 4.5 Monte Carlo simulated and Published PDD values for 10 MeV photons from a Varian machine

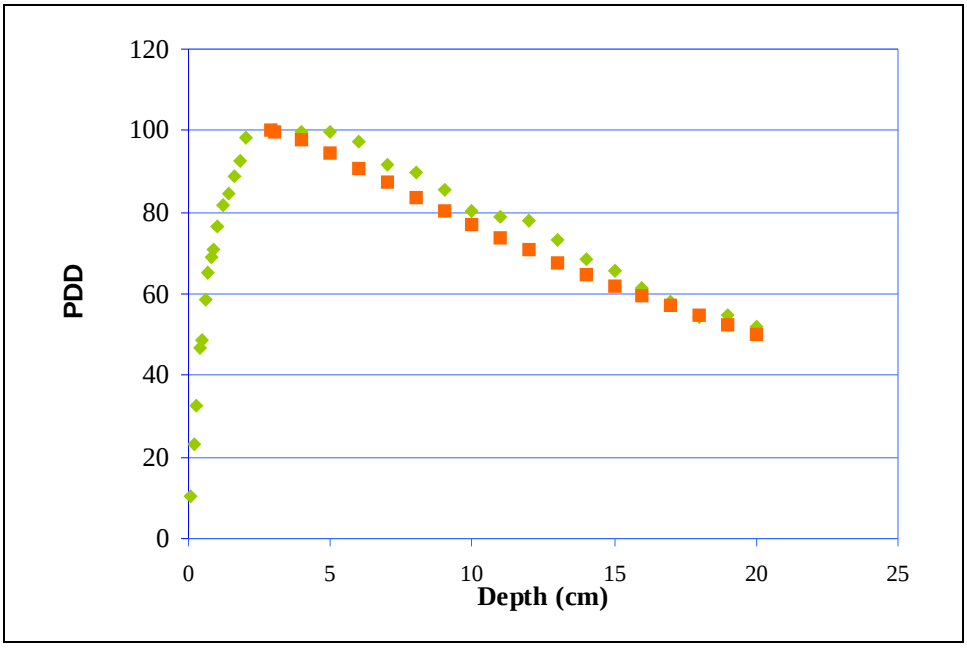

Figure 4.6 Monte Carlo simulated and Published PDD values for 15 MeV photons from Varian machine

4.4 Conclusions and future woks:

Before any new technology is implemented for clinical use the safety and appropriateness of the technology must be confirmed. For radiation machines such as linear accelerators the validation of dose calculation parameters and verification of stability of beam output must be undertaken carefully for a better treatment outcome. In the present investigations mathematical modeling of linear accelerator beams are carried out. Results of our investigations indicate that Monte Carlo simulation is an ideal tool for determining beam quality index for linear accelerators. Monte Carlo methods can also used to calculate the beam parameters for routine patient dose calculations and can be used to verify the experimentally determined dose calculation parameters.

Recent developments that fuse information from multiple imaging modalities such as CT and PET have enabled “image-guided” radiotherapy techniques, and have placed the role of computer simulation at the very center of radiation therapy. With the increasing reliance on computational tools, an increasing need is evident for the benchmarking and quality assurance of the computer models and codes that enable accurate simulations for the radiotherapy process. We believe that the present work can be considered as a part of the development of standardized Monte Carlo calculation algorithm benchmark data sets and an algorithm verification procedure.

CHAPTER 5

MODELING OF HOMOGENEOUS AND HETEROGENEOUS HUMAN BODY

Introduction:

Human body consists of bones and tissues with different physical and radiological properties. Air cavities such as oral cavity, sinuses and lung may exist in varying thickness. The first step in the radiation treatment planning process includes the derivation of patient anatomical information. This information is then used to determine the location of tumor and important normal tissue that could be affected by radiation treatment. Treatment Planning Systems (TPS) are used to determine the dose distribution that will result in the body from selected incident beams. Functionality of treatment planning system depends on the type of algorithms used in the planning process[81]. Different types of dose calculation algorithm are used in modern Treatment Planning Systems. Conventional TPS calculation models were based on a simple tabular representation of the dose distribution that was obtained directly from beam measurements. Standard isodose tables and charts are then prepared based on these measurements. These tables are used by TPS for patient dose calculations. Table based TPS required a lot of measured data tables. Measurements are usually taken in homogeneous water or water equivalent phantoms.

However, Human body is not homogeneous. The inhomogeineities can disturb the dose distribution. In order to achieve better tumor control it is essential to perform the dose calculations by considering these inhomogeineities also. Accurate calculation necessitates knowledge of thickness and composition of inhomogeineities and exact behavior of the incident radiation beam[82, 83]. Conventional treatment planning systems

cannot exactly predict the characteristics of dose distributions under the perturbation of inhomogeineities

In the present work we use Monte Carlo methods to study the effects of various inhomogeineities in the depth dose distributions.

5.1 Materials and Methods:

The Monte Carlo method has been described in detail in previous chapters.

Geometry Specifications:

The medium of irradiation was modeled as a block of tissue with cross section area 30× 30 cm^2 and a thickness of 3 cm (Figure 5.1). The region for dose estimation was modeled as a cylinder of radius 0.2 cm. This region was divided into small layers of thickness 0.05 cm thickness and total energy deposited in these regions was calculated. Three types of media were simulated as shown in figure 5.1

Case 1: In this case the radiation beam is incident on a Homogeneous medium of human adult tissue.

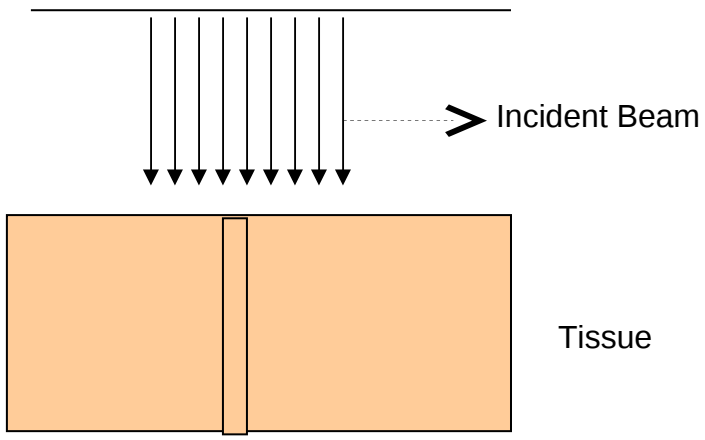

Case 2: In this case the beam is incident on a Heterogeneous medium of tissue and air. First layer is tissue followed by a layer of air .Third layer is again tissue. Such geometries areusually seen in the head and neck regions .

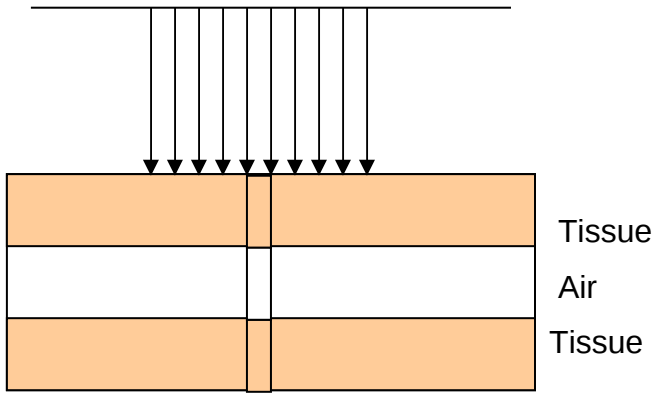

Case 3: In this case central layer is a bone.

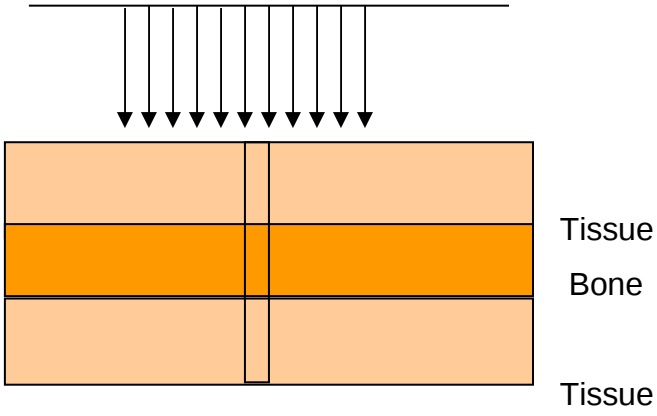

Figure 5.1 Geometries used to determine the variation of depth dose Characteristics with tissue in homogeneities.

Source Specifications

The incident beam was modeled as a surface source located directly in front and normal to the front face of the medium. The study was conducted for two prominent photon energies used for treatment.

(1) ^{60}Co beams

(2) 6MeV X-rays from a linear accelerator.

Material Specifications:

Three materials are used in our simulations. They are adult tissue, Bone and air. Composition and mass density of materials used in the present work are listed in Table 5.1

Total energy deposited in the small cylindrical regions was determined using an energy deposition tally available in the Monte Carlo code. PDD values are then calculated dividing the energy deposited in each cell by the value of maximum energy deposition. Number of particles transported in this modeling were 10^{7}.

Material	Density (gm/cc)	Composition and Mass fraction
Soft tissue	1	H (0.101) C (0.111) N (0.26) O (0.762)
Bone	1.41	H (0.064) C (0.263) N (0.039) O (0.436)
Air	0.001293	Na (0.001) Mg (0.001) P (0.06) S (0.03) Cl (0.001) K (0.001) C (0.00014) N (0.75519) O (0.23179) Ar (0.01288)

Table 5.1 _Material Specifications used in the work

5.2 Results:

Case1:

Depth Dose characteristics in homogeneous tissue medium for ^{60}Co and 6MeV Linac beams were studied. For both beams the dose increases at first and reaches a maximum and then decreases as the depth increases. The maximum dose is at 0.425cm depth for ^{60}Co beams. This depth is consistent with the published value. BJR published Standard Depth Dose values are only for depths beyond depth of maximum dose (d_{max}). No standard tables are available for doses at the surfaces because of measuring uncertainties. Observed surface dose from simulation is 17% of D_{max} dose. Percentage Depth Dose curves obtained from our simulations for ^{60}Co beams are shown in Figure 5.2(a)

For 6MeV photons the PDD values are obtained by transporting photons from a linear accelerator. The spectrum of photons is obtained from EGS nrc source code. Observed depth of maximum dose is 1.5 cm, which is consistent with published values. PDD pattern obtained for 6MeV photon is shown in Figure 5.2 (b). The surface dose for 6MeV photons is13 % of Dose maximum.

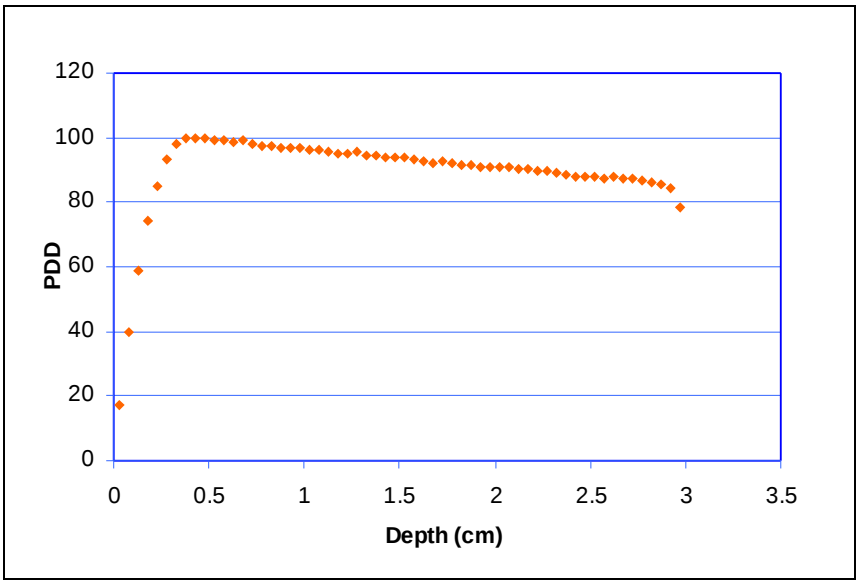

Figure 5.2 (a)PDD curves for ^{60}Co Beams in a homogeneous tissue medium

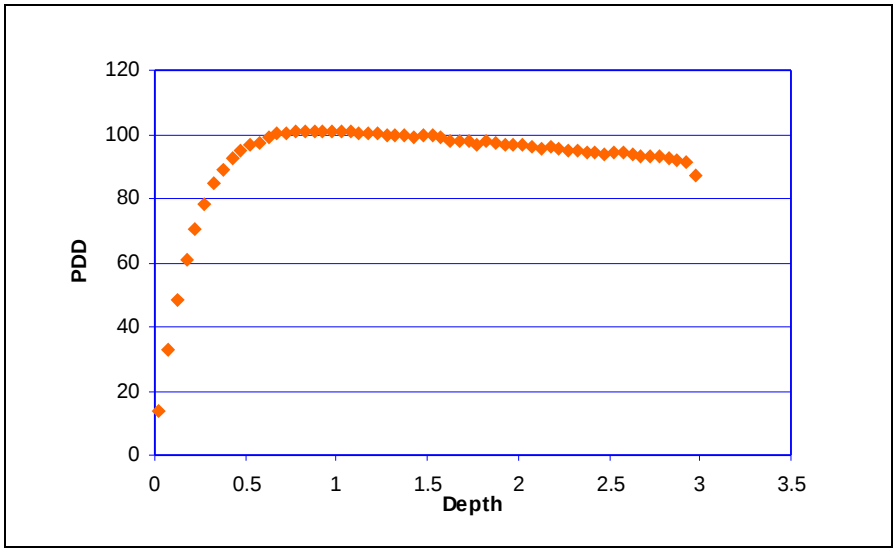

Figure 5.2 (b) PDD curves for 6MeV Beams in a homogeneous tissue medium

Case 2: Combination of tissue- Bone- Tissue medium:

The Percentage depth dose values obtained in our situation for ^{60}Co and 6MeV Linac beams are shown in figure 5.3(a) and 5.3(b).

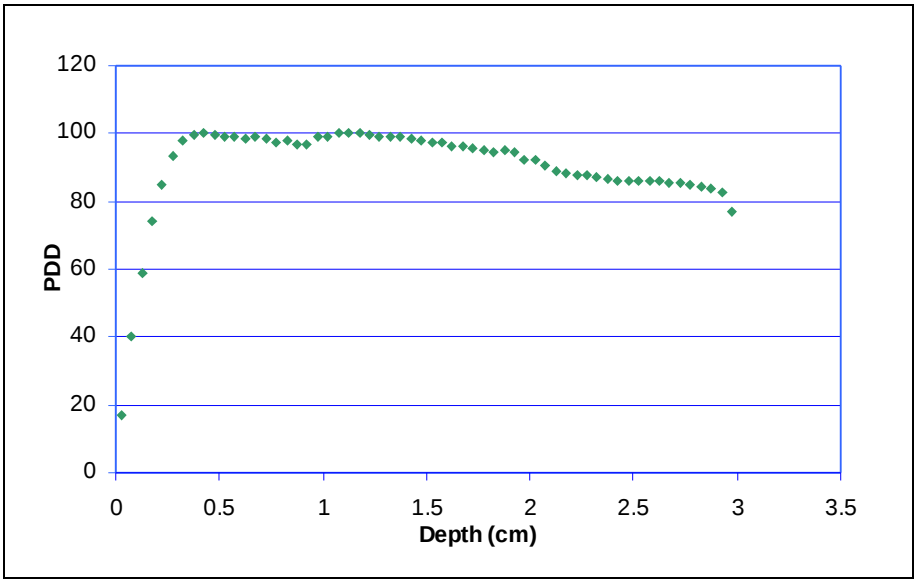

5.3(a) PDD curves for ^{60}Co Beams in tissue –Bone –Tissue medium

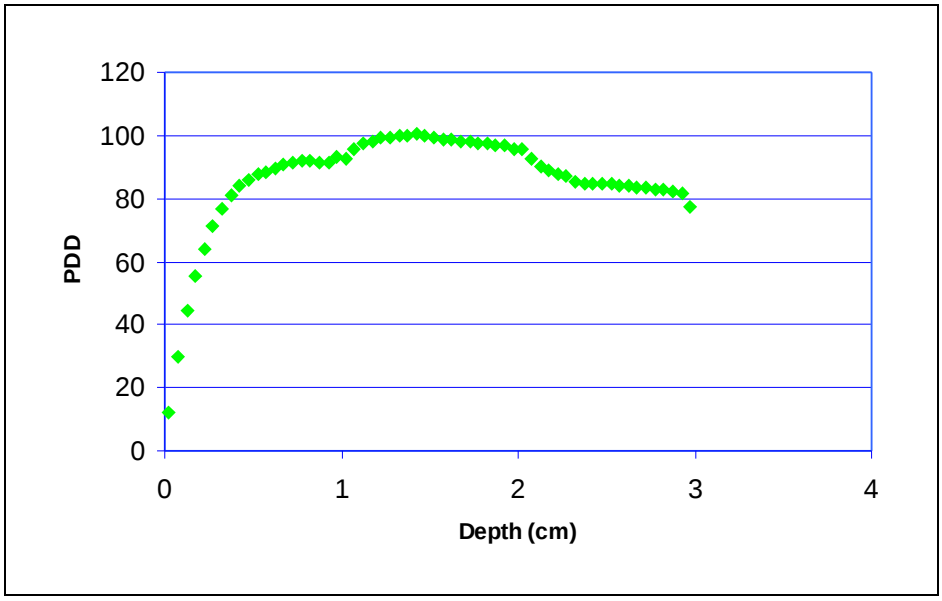

5.3(b) PDD curves for 6MeV Linac Beams in tissue –Bone –Tissue medium

In both cases (first layer of tissue) the dose pattern is exactly same up to 1cm thickness as that in the homogenous condition. However at the tissue bone interface the dose pattern is completely perturbed. The absorbed dose inside the bone layer is higher than that at the tissues (up to 5.4%). At the regions near the tissue bone interface the dose is above the D_{max} dose as specified in the homogeneous condition. The dose deposited at tissue bone interface is 2.2 to 4.1% higher than homogeneous conditions. PDD values in both conditions and percentage deviation from homogeneous conditions for ^{60}Co case are are shown in table 5.2. Same trend is also observed for 6MeV Linac beam

Depth	Homogeneous	Tissue-Bone-Tissue	
0.025	17.0	17.0	0.0
0.075	39.9	39.9	0.0
0.125	58.8	58.8	0.0
0.175	74.3	74.3	0.0
0.225	85.2	85.2	0.0
0.275	93.3	93.3	0.0
0.325	97.8	97.8	0.0
0.375	99.9	99.9	0.0
0.425	100.0	100.0	0.0
0.475	99.6	99.6	0.0
0.525	99.0	99.0	0.0
0.575	99.2	99.2	0.0
0.625	98.7	98.7	0.0
0.675	99.0	99.0	0.0
0.725	98.3	98.3	0.0
0.775	97.3	97.3	0.0
0.825	97.7	97.7	0.0
0.875	96.8	96.9	-0.2
0.925	96.6	97.1	-0.5
0.975	96.8	98.9	-2.2
1.025	96.3	99.2	-3.0
1.075	96.0	100.0	-4.1
1.125	95.4	100.3	-5.2
1.175	95.2	100.3	-5.4
1.225	95.0	99.7	-4.9
1.275	95.5	99.3	-4.0
1.325	94.6	99.0	-4.6
1.375	94.3	98.8	-4.8
1.425	94.1	98.2	-4.4
1.475	94.1	98.2	-4.4
1.525	94.1	97.6	-3.8
1.575	93.4	97.2	-4.1
1.625	92.9	96.2	-3.5
1.675	92.2	96.0	-4.1
1.725	92.5	95.7	-3.4
1.775	91.9	95.2	-3.6
1.825	91.4	94.5	-3.4
1.875	91.6	94.9	-3.6
1.925	91.0	94.5	-3.9
1.975	91.0	92.4	-1.6
2.025	90.7	92.2	-1.7
2.075	90.9	90.8	0.1
2.125	90.3	88.8	1.8
2.175	90.1	88.2	2.1

Table contd…..

2.225	89.5	87.8	2.0
2.275	89.8	87.9	2.1
2.325	88.9	87.0	2.2
2.375	88.2	86.3	2.2
2.425	88.1	86.2	2.2
2.475	87.9	86.1	2.1
2.525	87.7	85.8	2.2
2.575	87.6	85.8	2.1
2.625	88.1	86.2	2.1
2.675	87.5	85.6	2.2
2.725	87.2	85.3	2.1
2.775	87.0	85.1	2.2
2.825	86.4	84.5	2.2
2.875	85.5	83.7	2.2
2.925	84.4	82.6	2.1
2.975	78.6	76.9	2.1

Table 5.2 PDD values for ^{60}Co beams in homogeneous and Tissue bone tissue mediums

In the last layer of tissue (beyond 2 cm depth) the dose deposited is less than as expected from a homogeneous condition. Observed variation is up to 2.2 % less than the homogeneous conditions. The reason for this dose reduction is due to more attenuation of radiation in the previous bone layer. The electron density in bone is more than in tissue. As a result the probability of Compton interaction will be more at bone than in tissue causing more attenuation.

Case 3:Combination of Tissue -Air-Tissue medium:

In this case the dose absorbed at the first layer of tissue is exactly same as that of homogenous conditions. Observed dose deposition in the air layer is very small. At the first tissue air interface the deviation from homogeneous condition is up to 7%. PDD values at other points in the air medium show variation up to 95.3% than the homogeneous condition. This much variation is due to the fact that absorbed dose in air will be much less than that in tissue due to the difference in their densities. Interestingly It is

also observed that a build up condition occur at the second air -tissue interface. In this region the PDD values are only 20.6 to 42.09 at the first few Millimeters and increases up to 93.5 % of D_{max} values (Figure 5.4).

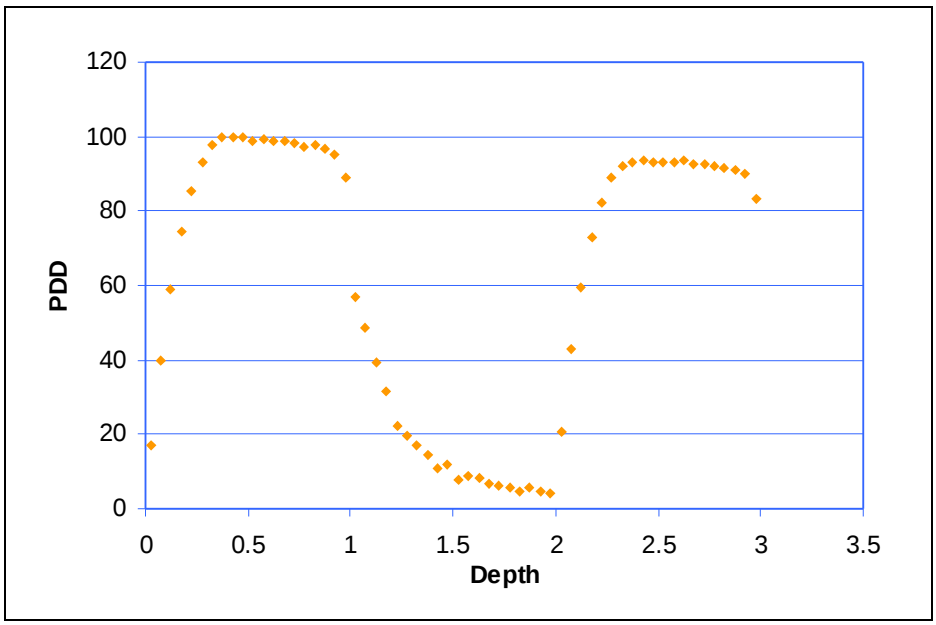

Figure 5.4 PDD curves for ^{60}Co Beams in Tissue –Air –Tissue medium

PDD values for Tissue Air Tissue medium and corresponding deviations from the homogenous conditions are given shown in table 5.3. In air the absorption is very less due to the less density and the tissues beyond the air cavity will get very high dose. The observed deviation is up to 77% than expected from the homogenous condition and at shallower depths the deviation is about 6%.

Depth	Homogeneous	Tissue-Air-Tissue	% Deviation

0.025	17.0	17.0	0.0
0.075	39.9	39.9	0.0
0.125	58.8	58.8	0.0
0.175	74.3	74.3	0.0
0.225	85.2	85.1	0.0
0.275	93.3	93.3	0.0
0.325	97.8	97.8	0.0
0.375	99.9	99.8	0.0
0.425	100.0	100.0	0.0
0.475	99.6	99.6	0.0
0.525	99.0	99.0	0.0
0.575	99.2	99.2	0.0
0.625	98.7	98.7	0.0
0.675	99.0	99.0	0.0
0.725	98.3	98.3	0.0
0.775	97.3	97.3	0.0
0.825	97.7	97.6	0.1
0.875	96.8	96.5	0.3
0.925	96.6	95.3	1.3
0.975	96.8	89.1	7.9
1.025	96.3	57.1	40.7
1.075	96.0	48.4	49.6
1.125	95.4	39.6	58.5
1.175	95.2	31.8	66.6
1.225	95.0	22.4	76.4
1.275	95.5	19.7	79.4
1.325	94.6	17.0	82.1
1.375	94.3	14.4	84.7
1.425	94.1	10.8	88.6
1.475	94.1	11.8	87.4
1.525	94.1	8.0	91.5
1.575	93.4	8.6	90.8
1.625	92.9	8.3	91.1
1.675	92.2	6.5	92.9
1.725	92.5	6.2	93.3
1.775	91.9	5.7	93.8
1.825	91.4	4.9	94.6

Table Contd……

1.875	91.6	5.8	93.7
1.925	91.0	4.6	94.9
1.975	91.0	4.3	95.3
2.025	90.7	20.6	77.3
2.075	90.9	42.9	52.8
2.125	90.3	59.6	34.0
2.175	90.1	72.8	19.3
2.225	89.5	82.1	8.3
2.275	89.8	89.2	0.6
2.325	88.9	92.1	-3.5
2.375	88.2	93.1	-5.5
2.425	88.1	93.5	-6.1
2.475	87.9	93.3	-6.1
2.525	87.7	93.0	-6.0
2.575	87.6	93.0	-6.2
2.625	88.1	93.4	-6.0
2.675	87.5	92.8	-6.0
2.725	87.2	92.5	-6.1
2.775	87.0	92.3	-6.1
2.825	86.4	91.7	-6.1
2.875	85.5	90.8	-6.2
2.925	84.4	89.8	-6.3
2.975	78.6	83.5	-6.3

Table 5.3 PDD values for ^{60}Co beams in homogeneous and Tissue- Air-Tissue mediums

5.3 Conclusions and future works:

Dose measurements at the interface between two media are impossible to measure by conventional measurements. The interface effects in the presence of inhomogeineities are a common dosimetric problem encountered in routine treatment planning process[80]. Treatment planning systems employing pencil beam algorithms are incapable of handling such situations[82]. The collapsed cone algorithms are generally

better in predicting the interface effects but changes in the scatter distribution relative to water in the presence of homogeneities are not modeled accurately[83, 84].

Treatment planning systems express dose distributions in terms of so-called isodose lines connecting points of equal dose, and superimposed on CT sections through the patient under study. For an extremely heterogeneous anatomy (eg head and neck region) with the pencil-beam algorithm widely employed in commercial radiotherapy treatment planning systems show a smooth isodose distribution. However true dose distributions of such a narrow photon beam in heterogeneous terrain will be grossly distorted. Introduction of Monte-Carlo simulation into the patient dose calculation systems will solve such problems and provide more accurate dose distributions.

We believe that our work is a stepping-stone for the development of a Monte Carlo based Dose computation system to improve the clinical outcome of radiotherapy. Future works will be focused on the adaptation of Monte-Carlo method to model today's increasingly complex treatment delivery techniques e.g. using MLCs to shape fields to the tumor shape and to modulate the fluence across the beam to reduce the irradiation of so-called organs at risk. Future works may also focus on the development of a Monte Carlo based TPS to solve the present dilemmas associated with tissue inhomogeineities to improve cancer treatment outcomes.

CHAPTER 6

SUMMARY

Mathematical Modeling and simulations offer very important tools used in scientific research and techniques for understanding physical laws and phenomena, measuring methods and processes and device operations and instrument execution. Mathematical Modeling has many applications in nuclear physics such as design of nuclear reactor and particle accelerator. The objective of the present work is to establish the feasibility of mathematical modeling of the radiation transport for the medical application of nuclear radiations. *With this objective we have undertaken to investigate the feasibility of Monte Carlo methods for the mathematical modeling in radiotherapy.* The results of our work were presented in the thesis as five chapters of this thesis.

A thorough literature survey had been conducted and is given in the introductory chapter of the thesis.

In chapter 2 details of mathematics of radiation transport had been presented.

In chapter 3 mathematical modeling of a radiotherapy machine commonly used for cancer treatment in India is described. A detailed study of the radiation beam characteristics had been undertaken and results were presented. Work also had been conducted to obtain the dosimetric parameters important for patient dosimetry by mathematical modeling of the telecobalt machine and the measuring systems. Parameters obtained from the simulations were compared with experimental values. The results are promising and consistent with the experimental values.

In Chapters 4 results of mathematical modeling a linear accelerator had been presented. Results of our investigations indicate that Monte Carlo simulation is an ideal tool for determining beam quality index for linear

accelerators. The experimental validation of the Monte Carlo simulations are done by comparing the calculated results with those obtained by experimental measurements. Monte Carlo methods can also be used to calculate the beam parameters for routine patient dose calculations and can be used to verify the experimentally determined dose calculation parameters.

In chapter 5 we presented the simulation results of radiation transport through different tissue inhomogeineities. Prediction the dose at the interfaces and regions below the interfaces are a challenge for the radiation physicist as the measurements of dose at the interface between two media are impossible by conventional methods. The present work clearly shows that Monte Carlo methods can accurately predicts the dose perturbations due to tissue inhomogeineities. We believe that the present work offers a guideline and comparison tool for verification treatment planning systems.

Finally, it is apparent that technology is continuously getting more complex to adapt to patient specific treatments in the field of medical physics. We believe that our work is a stepping-stone for the development of a Monte Carlo based Dose computation system to improve the clinical outcome of radiotherapy. Future works will be focused on the adaptation of Monte-Carlo method to model today's increasingly complex treatment delivery techniques e.g. using Multi leaf collimators to shape fields to the tumor shape and to modulate the fluence across the beam to reduce the irradiation of so-called organs at risk. Future works may also focus on the development of a Monte Carlo based treatment planning systems to solve the present dilemmas associated with tissue inhomogeineities to improve cancer treatment outcomes.

Summarizing, We believe that this thesis provides the knowledge that was required to improve the accuracy of treatment planning calculations to reach the ultimate goal of a radiation treatment - a better quality of life for cancer patients.

BIBLIOGRAPHY

1 Walstam. Medical radiation physics in Europe, a historical review on radio therapeutic applications in Radiation Oncology,"1895-1995", a century of progress and achievements. ESTRO, Leuven, 1995.

2 Urtasun. Technology improvement and local tumor control In Teletherapy, present and future. Proceedings of the 1996 summer school, American Association of Physicists in Medicine, Maryland, 1-16, 1996.

3 Suit. Local control and patient survival. Int J Radiat Oncol Biol Phys 1992, 23: 653-660.

4 KHAN FM. The Physics of Radiation Therapy, 3rd edition. Lippincott, Williams and Wilkins, Baltimore, MD 2003.

5 JOHNS HE, CUNNINGHAM JR. The Physics of Radiology. Thomas-Springfield, IL, 1984.

6 AMERICAN ASSOCIATION OF PHYSICISTS IN MEDICINE, Comprehensive QA for radiation oncology. Report of AAPM Radiation Therapy Committee Task Group 40. Med Phys1994, 21**:** 581–618.

7 Boyer AL, Schultheiss T. Effects of dosimetric and clinical uncertainty on complication-free local tumor control. Radiother Oncol 1988,11: 65-71.

8 Institute of Physics and Engineering in Medicine, Physics aspects of Quality control in Radiotherapy, Report 81, edited by: Mayles WPM, Lake R, McKenzie A, Macaulay EM, Morgan HM, Jordan TJ and. Powley S K , IPEM, York, 2000

9 Suit HD, Becht J, Leong J, Stracher M, Wood WC, Verhey L and Goitein M. Potential for improvement in radiotherapy. Int J Radiat. Oncol Biol Phys1988, 44: 777-786.

10 Van Dyk, Wong E, Craig J, Batista JJ. Uncertainty analysis: a guide to optimization in radiation therapy. Radiother Oncol (Suppl1)1998, 48: 151.

11 Fenwick JD, Nahum AE. Impact of dose distribution uncertainties on rectal NTCP modeling, Uncertainty estimates. Med Phys 2001, 28: 560-569.

12 Wong E, Van Dyk, Battista JJ , Barnett RB, Munro PN. Uncertainty analysis: A guide to optimization in radiation treatment planning. Proceedings of XIIth International Conference on the Use of Computers in Radiotherapy, Medical Physics Publishing, Madison, 259, 1997.

13 Lujan AE, Ten Haken RK, Larsen EW, Balter JM. Quantization of setup uncertainties in 3-D dose calculations. Med Phys 1999, 26: 2397-2402.

14 Van Herk M, Remeijer P, Lebesque JV. A tool for evaluation the robustness of clinical treatment plans. Int J Radiat Oncol Biol Phys 2000, 48:192.

15 Schilstra C, Meertens H. Calculation of the uncertainty in complication probability for various dose-response models, applied to the parotid gland. Int J Radiat Oncol Biol Phys 2001, 50: 147-158.

16 Steel GG, Ed.2002 Basic clinical radiobiology. London, Arnold.

ISBN 0 340 80783 0.

17 Brahme A, Chavaudra J, Landberg T, McCullough EC, Nüsslin F,. Rawlinson JA, Svensson G, Svensson H. Accuracy requirements and quality assurance of external beam therapy with photons and electrons. Acta Oncol (Supp l) 1988, 27: 19

18 Mijnheer BJ, Battermann JJ, Wambersie A. What degree of accuracy is required and can be achieved in photon and neutron therapy. Radiother Oncol 1987, 8: 237-252.

19 International Commission on Radiological Units, Determination of absorbed dose in a patient irradiated by beams of X and gamma rays in radiotherapy procedures, Report 24, ICRU, Washington, 1976.

20 Mackie TR, Reckwerdt P, McNutt T, Gehring M, Sanders C. Photon beam dose computations in Teletherapy: present and future. Proceedings of the AAPM summer school, American Association of Physicists in Medicine, Maryland, 103,1996.

21 Ahnesjo, Aspradakis MM. Dose calculations for external photon beam in radiotherapy. Phys Med Biol 1999, 44: R99-R155.

22 Andreo P, Burns DT, Hohlfeld K, Huq MS, Kanai T, Laitano F, Smyth VG , Vynckier S. Absorbed dose determination in external beam radiotherapy: An international code of practice for dosimetry based on standards of absorbed dose to water. In: Technical Report Series 398, IAEA , Vienna 2000.

23 Hohlfeld K. Procedures for absorbed dose determination in radiology by the ionization method. In: Dosimetry in Radiotherapy (IAEA-SM-298/31) *Vol*. 1, 13–22, IAEA, Vienna. 1988.

24 Review of Radiation Oncology Physics: A Handbook for Teachers and Students: (Ervin B. Podgorsak Editor), Educational Reports Series, International Atomic Energy Agency, Vienna, Austria. May 2003.

25 MIJNHEER A, BRIDIER C, GARIBALDI K, TORZSOK J, VENSELAAR. Monitor Unit Calculation For High Energy Photon Beams - Practical Examples, ESTRO booklet (First edition). ESTRO, Brussels, Belgium 2001.

26 AMERICAN ASSOCIATION OF PHYSICISTS IN MEDICINE, AAPM's TG-51 protocol for clinical reference dosimetry of high-energy photon and electron beams, Med Phys1999, 26**:** 1847–1870.

27 INSTITUTE OF PHYSICAL SCIENCES IN MEDICINE, Code of practice for high-energy photon therapy dosimetry based on the NPL absorbed dose calibration service. Phys Med Biol 1990, 35:1355–1360.

28 SEUNTJENS JP. Absorbed-dose beam quality correction factors for cylindrical chambers in high-energy photon beams. Med Phys 2000,27**:** 2763–2779.

29 KASE KR, BJARNGARD BE, ATTIX FH. The Dosimetry of Ionizing Radiation. Academic Press, San Diego, CA 1985.

30 SAUTOY AR. The UK primary standard calorimeter for photon-beam absorbed dose measurement. Phys Med Biol 1996,41:137.

31 Nahum AE. Water/air mass stopping-power ratios for mega voltage photon and electron beams. Phys Med Biol 1998*,* 23**,** 24-38

32 Rogers DWO, Bielajew AF. Monte Carlo techniques of electron and photon transport for radiation dosimetry. In: The dosimetry of ionizing radiation (Kase KR, Bjarngard BE and Attix FH eds.) Vol. III, 427-539, Academic Press, San Diego, 2000.

33 Law AM, Kelton D. Simulation Modeling and Analysis, 3rd Ed, McGraw-Hill, New York, 2000.

34 John S, Carson II. Introduction to modeling and simulation. Proceedings of the Winter Simulation Conference (Chick S, Sanchez PJ, Ferrin D, Morrice DJ Eds.), New York, 2003.

35 O'Dell RD, Alcouffe RE. Transport Calculations for Nuclear Analysis-Theory and Guidelines for Effective Use of Transport Codes. Los Alamos National Laboratory report, LA-10983-MS, 1987.

36 Andreo P. Monte-Carlo techniques in medical radiation physics. Phys Med Biol 1991, 36: 861-920.

37 Petti P L, Goodman MS, Mohan TAR. Investigation of buildup dose from electron contamination of clinical photon beams. Med Phys1983, 10: 18-24.

38 Yang et al. Modeling of electron contamination in clinical photon beams for Monte Carlo dose calculation. Phys Med Biol 2004, 49: 2657-2673.

39 Rogers DWO, Ewart GM, Bielajew AF, Van Dyk G. Calculation of Electron Contamination in a ^{60}Co Therapy Beam. In: Proceedings of the IAEA International Symposium on Dosimetry in Radiotherapy Vol. 1, IAEA, Vienna, 303 – 312,1988.

40 Kase K, Nizin PS. A method of measuring the primary dose component in high-energy photon beams. Med Phys 1988,15: 683-685.

41 Nizin PS. Geometrical aspects of scatter-to-primary ratio and primary dose. Med Phys 1991,18: 153-160.

42 Udale M. Monte Carlo calculations of electron beam parameters for three Philips linear accelerators. Phys Med Biol1992, 37: 85–105.

43 Rogers DWO, Faddegon BA, Dhg GX, Ma C, Wei S, Mackie TR. BEAM: A Monte Carlo code to simulate radiotherapy treatment units. Med Phys 1995, 22: 503-524.

44 Bjarngard BE, Paul Vadash, Analysis of central-axis doses for high-energy X rays. Medical Physics 1995, 22: 1191-1195

45 DeMarco TD, Solberg RE, Wallace, Smathers JB. A verification of the Monte Carlo code MCNP for thick target Bremstrahlung calculations. Med Phys1995, 22: 11-16.

46 The British Journal of Radiology, Supplement 25. Br J Radiology 1996.

47 Love PA, Lewis DG, Al-Affan IAM, Smith CW. Comparison of EGS4 and MCNP Monte Carlo codes when calculating radiotherapy depth doses. Phys Med Biol 1998,51.

48 DeMarco TD, Solberg, Smathers JB. A CT-based Monte Carlo dosimetry tool for dosimetry planning and analysis. Med Phys1998, 25: 1-11.

49 Hubbell. Review and history of photon cross-section calculations. Phys Med Biol 1998, 51:13.

50 Difilippo et al. Forward and adjoint methods for radiotherapy planning. Med Phy 1998, 25: 1702-1710.

51 Ulanovsky, Eckerman KF. Modifications to the ORNL Phantom Series in Simulation of the Responses of Thyroid Detectors. Radiation Protection Dosimetry 1998, 79: 429-431.

52 Mora, Maio A, Rogers DWO. Monte Carlo simulation of a typical ^{60}Co therapy source. Med Phys 1999, 26: 2494-2502.

53 Wung, Michael Lovelock, Chen-Shou Chu. Experimental verification of a CT-based Monte Carlo dose-calculation method in heterogeneous phantoms. Med Phys 1999, 26: 2626-2634.

54 Lewis RD et al. An MCNP-based model of a linear accelerator x-ray beam. Phys Med Biol1999, 44: 1219-1230.

55 Sheikh DB, Rogers DWO, Carl K Ross, Seuntjens JP. Comparison of measured and Monte Carlo calculated dose distributions from the NRC linac. Medical Physics 2000, 27: 2256-2266.

56 Biju K, Nagarajan PS. Normalized organ doses and effective doses to a reference Indian adult male in conventional medical diagnostic x-ray examinations. Health Phys 2006, 90: 217-22.

57 Rogers DWO. Monte Carlo Techniques for Primary Standards of Ionizing Radiation and for Dosimetry Protocols. Med Phys 2003, 30:521.

58 Reynaert N, Palmans H, Thierens H, Jeraj R. Parameter dependence of the MCNP electron transport in determining dose distributions. Med Phys 2002,29: 2446-54.

59 Aleissa A, Khalid E. Energy response simulation of 4 gamma ionization chambers using Monte Carlo technique. Med Phys 2002 – 29: 2840-2844.

60 Nutbrown et al. Evaluation of factors to convert absorbed dose calibrations from graphite to water for the NPL high-energy photon calibration service. Phys Med Biol 2002, 47: 441-454.

61 Damilakis, Antonis Tzedakis, Liana Sideri, Kostas Perisinakis, Stamatelatos, Nicholas Gourtsoyianni. Normalized conceptus doses for abdominal radiographic examinations calculated using a Monte Carlo technique. Med Phys 2002, 29:2641-2648.

62 Bohm TD, DeLuca, DeWerd PM. Brachytherapy dosimetry of ^{125}I and ^{103}Pd sources using an updated cross section library for the MCNP Monte Carlo transport code. Med Phy 2003, 30.

63 Teimouri Sichani. Monte Carlo dose calculations for radiotherapy machines, Theratron 780-C Teletherapy case study. Phys Med Biol. 2004,49: 807-818.

64 Brian Wang et al. Adjoint Monte Carlo method for prostate external photon beam treatment planning, an application to 3D patient anatomy. Phys Med Biol 2005, 50: 923-935.

65 Brian Wang, George, Tim Goorley, Ahmet Bozkurt. Issues related to the use of MCNP code for an extremely large voxel model Vip-man, In: The Monte Carlo method, versatility unbounded in a dynamic computing world,17–21, Chattanooga, Tennessee, 2005,.

66 Rogers DWO, R Mohan - Questions for comparison of clinical Monte Carlo codes. In: The proceedings of The Use of Computers in Radiotherapy, XIII th International Conference, UK, 2004.

67 Srinath Reddy, Bela Shah, Cherian Varghese, Anbumani Ramadoss. Responding to the threat of chronic diseases in India. The Lancet 2005, 366:1744-174.

68 Sarin Rajiv. Indian national cancer control programme: Setting sight on shifting targets. Journal of Cancer Research and Therapeutics 2005,1.

69 McKenzie AL. "Cobalt-60 gamma-ray beams". Br J Radiol 1996, Supplement 25: 46-5 1.

70 Hubbell JH, Seltzer SM. Tables of X-Ray Mass Attenuation Coefficients and Mass Energy-Absorption Coefficients from 1 keV to 20 MeV for Elements *Z* = 1 to 92 and 48, Additional Substances of

Dosimetric Interest, NISTIR 5632, National Institute of Standards and Technology, UK,1999.

71 Godden TJ. Gamma radiation from cobalt 60 teletherapy Units. Br J Radiology 1983, Supplement 17: 45-49.

72 David I Thwaites et al. Back to the future: the history and development of the clinical linear accelerator. Phys Med Biol 2006, 51 R343-R362.

73 Knoos. The dosimetric verification of a pencil beam based treatment-planning system. Phys Med Biol1994, 39: 1609-162.

74 Knoos A, Ahnesjo P, Nilsson, Weber L. Limitations of a pencil beam approach to photon dose calculations in lung tissue. Phys Med Biol1995, 40: 1411-1420.

75 Briesmester JF. MCNP –A general Monte Carlo N-Particle transport Code, Los Alamos National Laboratory Report, LA-12625-M, 1993.

76 McKenzie Alan. What is the explanation for the changes to ^{60}Co tissue – air- ratios in BJR Supplement 25. Phys Med Biol 1997, 42: 1055-1064

77 Karzmark CJ, Nunan CS, Tansbe E. Medical Electron Accelerators MC Graw –Hill, New York, NY, 1993.

78 Verhaegen Frank et al. Monte Carlo modeling of external radiotherapy photon beams. Phys Med Biol 2003, 48: R107-R164.

79 Sheikh-Bagheri, Rogers DWO. Calculation of nine mega voltage photon beam spectra using the BEAM Monte Carlo code. Medical Physics 2002, 29: 391 – 402.

80 http:// www.irs.inms.nrc.ca/inms/irs/irs.html.

81 AMERICAN ASSOCIATION OF PHSICISTS IN MEDICINE. Quality Assurance for Clinical Radiotherapy Treatment Planning, AAPM Task Group 53 Report. Med Phys 1998, 25:1773 – 1829.

82 Westermann BJ, Mijnheer, Van Kleffens HJ. Determination of the accuracy of different computer planning systems for treatment with external photon beams. Radiother Oncol 1984,1 : 339-347.

83 Ahnesjo. Collapsed Cone convolution of radiant energy for photon dose calculation in heterogeneous media. Med Phys 1989,16:577-592.

84 Ahnesjo, Knoos T, Montelius A. Application of the convolution method for calculation of output factors for therapy photon beams. Med Phys 1990,19: 295-301.

85 Martin A, Ebert, Nigel A, Spry. Dose perturbation by air cavities in mega voltage photon beams: Implications for cavity surface doses. Australasian Radiology 2001, 45: 205-210.

86 Brahme A. Accuracy requirements and quality assurance of external beam therapy with photons and electrons. Acta Oncol1988, suppl.1

87 Makie. Generation of Photon energy deposition kernels using Egs4 Monte Carlo code. Phy med Biol 1988, 33:1-20

88 Cossairt. Radiation Physics for Personnel and Environmental Protection. Fermi National Accelerator Laboratory, FERMILAB-TM-1834 (website http://lss.fnal.gov/archive/1999/tm/TM-1834intro.pdf)

89 Parthasaradhi K, Prasad S G, Rao B M, Lee Y, Ruparel R, R Garces. Investigation on the reduction of electron contamination with a 6-MV x-ray beam. Med Phys 1989,16: 123 – 125.

90 Aitken, Henry W H. Spectra of the Internally Scattered Radiation from large ^{60}Co Sources used in Teletherapy. Int'l J of Applied Radiation and Isotopes 1964, 15: 713 – 724.

91 Rogers DWO. Fifty years of Monte Carlo simulations for medical physics. Phys Med Biol 2006, 51 R287-R301.

92 Vlamynck KD, Palmans H, Verhaegen F, Wagte CD, Neve WD, Thierens H. Dose measurements compared with Monte Carlo simulations of narrow 6 MV multileaf collimator shaped photon beams. Med Phys 1999, 26: 1874-1882.